Validation of ISCCP Cloud Detections

WILLIAM B. ROSSOW

NASA Goddard Institute for Space Studies, New York, New York

LEONID C. GARDER

Columbia University, New York, New York

(Manuscript received 10 June 1992, in final form 12 May 1993)

ABSTRACT

The International Satellite Cloud Climatology Project (ISCCP) began in 1983 to collect and analyze weather satellite datasets to produce a new global cloud climatology as part of the World Climate Research Programme. The first step of the analysis is detection of the presence of clouds at each location and time by a series of tests on the space/time variations of infrared and visible radiances. This paper describes the validation of the ISCCP cloud detections by verifying the accuracy of the inferred clear-sky radiances. Comparison of retrieved surface temperatures to other measurements shows that bias errors are <2 K and random errors are about 2 K for sea surface (monthly means at 280-km scales) and that bias errors are <2 K and random errors are about 4 K for land surfaces (3 hourly at 280-km scale). Bias errors over a few persistently cloudy locations are sometimes −(2–4) K and over winter sea ice may be about +2 K. Surface reflectances are confirmed to be within 3% of other measurements and models for ocean, except for sun glint geometries, and to be within 3%–5% for land surfaces. Sufficiently accurate validation data are not available for visible reflectances of sea ice and snow-covered land, but some tests of specific cases suggest that errors are ~10%. These errors in clear-sky radiances suggest uncertainties in the ISCCP cloud detections of about 10% with a small (3%–6%) negative bias over land. Some specific regions exhibit both larger rms uncertainties and somewhat larger biases in cloud amount approaching 10%. ISCCP cloud detections are more in error over the polar regions than anywhere else. Based on comparisons with an analysis of radiances measured at other wavelengths, the ISCCP analysis appears to miss 15%–25% of the clouds in summer but only 5%–10% of the winter clouds.

1. Introduction

The International Satellite Cloud Climatology Project (ISCCP) was established in 1982 to produce a globally uniform satellite cloud climatology (Schiffer and Rossow 1983). Imaging radiometers on weather satellites, both geostationary and polar orbiting, measure radiation in a number of discrete spectral bands; the two bands common to all satellites are at visible (VIS $\approx 0.65 \pm 0.15$ μm) and infrared (IR $\approx 11 \pm 1$ μm) wavelengths. The ISCCP cloud climatology is obtained from an analysis of a sampled and calibrated version of these radiance data, called stage B3 (Schiffer and Rossow 1985). The first step in the analysis is to determine whether clouds are present at each time and place. The ISCCP cloud detection method, together with the supporting statistical evidence used to design and test the sensitivity of the method, is described in detail by Rossow and Garder (1993). The subject of this paper is validation of the ISCCP cloud detections.

Clouds are detected by the radiance variations that they cause either spatially or temporally. Clouds that do not alter the IR or VIS radiances enough remain undetected. Radiance changes are determined by comparison of the measured radiances at each place and time with estimates of the radiance values that represent clear conditions. The algorithm for estimating clear radiances is briefly described in section 2a, along with its sensitivity to changes in the test parameter values. Since the atmosphere is nearly transparent at IR and VIS wavelengths, clear radiances are determined primarily by the properties of the surface (temperature and reflectance, respectively). Thus, cloud detections can be verified by comparing the surface properties inferred from the clear radiances with other measurements of the same or related surface properties (cf., Rossow et al. 1989a; Rossow et al. 1989b). The radiance dataset and the radiative transfer model used to retrieve surface temperature and visible reflectance are described in section 2b. The comparison datasets are described in section 2c.

The comparisons (section 3) determine two kinds of cloud detection error. Bias errors in the clear radiances cause either false cloud detections or detection failures, which lead to biases in cloud amounts. Random errors in the clear radiances also cause detection errors; but, if the magnitude of the clear radiance errors

Corresponding author address: William B. Rossow, NASA Goddard Institute of Space Studies, 2880 Broadway, New York, NY 10025.

is no larger than assumed by the algorithm's detection thresholds, then there is no systematic effect on cloud amounts because occasional false detections will be offset by some detection failures. If, on the other hand, the clear radiance errors are significantly smaller or larger than assumed, the cloud detections are either too infrequent or too frequent and the cloud amounts are biased low or high. A summary of estimated detection errors is presented in section 4.

The second part of the validation of ISCCP cloud amounts is presented in a companion paper (Rossow et al. 1993), which concerns the conversion of cloud detections (spatial frequency of occurrence) into cloud cover fraction. By counting the relative number of image pixels (instrument fields of view) that contain some cloud, the ISCCP procedure determines cloud fraction over larger areas from a sample of smaller subareas. Comparisons of ISCCP cloud amounts with other values determined at much higher spatial resolution indicate how sampling and pixel size affect estimates of cloud cover. This companion paper also presents a detailed comparison of the ISCCP cloud climatology with three other climatologies, one based on surface observations and two on satellite measurements.

2. Cloud detection algorithm and datasets

a. Cloud detection steps

The ISCCP cloud detection procedure is applied to each month of satellite data and consists of five steps (Rossow and Garder 1993):

1) space contrast test (applied to individual IR images),
2) time contrast test (three consecutive IR images at constant diurnal phase),
3) cumulation of space/time statistics (both IR and VIS images),
4) construction of clear-sky composites for both IR and VIS (once every 5 days at each diurnal phase and location),
5) radiance threshold (both IR and VIS images).

The first test classifies as cloudy all image pixels that are much colder (low IR radiance) than the warmest value in small spatial domains. It is a spatial contrast test because the warmest pixel is not classified as either clear or cloudy but remains unclassified. The second test classifies as cloudy all pixels that have sharply lower IR radiances at the same location as compared with values one day earlier or later and classifies as clear all pixels that show little variation of IR radiance over one-day intervals. The results of the two time comparisons are combined as shown in Fig. 1a. To avoid confusion with diurnal variations of surface temperatures, this test is performed separately at each time of day. The results of the space and time contrast tests are combined as shown in Fig. 1b. Note that an image

TIME TEST LOGIC

TOMORROW'S TEST \ YESTERDAY'S TEST	CLOUDY	UNDECIDED	CLEAR
CLOUDY	CLOUDY	CLOUDY	MIXED
UNDECIDED	CLOUDY	UNDECIDED	CLEAR
CLEAR	MIXED	CLEAR	CLEAR

COMBINED SPACE-TIME TESTS LOGIC

TIME TEST \ SPACE TEST	CLOUDY	UNDECIDED
CLOUDY	CLOUDY	CLOUDY
UNDECIDED	CLOUDY	UNDECIDED
MIXED	MIXED	MIXED
CLEAR	MIXED	CLEAR

FIG. 1. Logic tables (a) to combine the results of the time contrast test comparing the "today" image with the "yesterday" and "tomorrow" images and (b) to combine the results of the space contrast test and the time contrast test. Undecided means that no decision (cloudy or clear) is made for a particular scene. Mixed indicates contradictory decisions by different tests. All comparisons are performed separately for each diurnal phase.

pixel is labeled clear only when it exhibits low variability in *both* space and time. The third step collects other statistics on the variations of the IR and VIS radiances over larger spatial and temporal domains. These statistics are compared in the fourth step, along with the results from the first two tests (number of clear pixels and average clear radiance), to estimate values of clear IR and VIS radiances for each location and diurnal phase, once every five days. In the final step, the original IR and VIS radiances at each location and time are compared with the inferred clear values to determine the magnitude and sign of the differences. If the observed radiances in a pixel differ from the clear-sky values (lower IR and/or higher VIS) by more than the estimated uncertainty of the clear-sky values (Table 1), the pixel is classified as cloudy. A subset of these pixels, with radiance values close to the values dividing clear from cloudy are referred to as marginally cloudy (Fig. 2). All other pixels are classified as clear.

The fundamental premise of this cloud detection method is that clouds cause the largest space and/or time variations of the IR and/or VIS radiances: the

TABLE 1. Cloud detection radiance thresholds used for different surface types. IR thresholds are given in kelvins and VIS thresholds are given in percent scaled radiances.

	IR threshold	VIS threshold
Open ocean	2.5	3.0
Near-coastal ocean, lakes	4.0	3.0
Ice covered water	4.0	12.0
Land	6.0	6.0
High or rough topography	8.0	6.0
Snow-covered land	6.0	12.0

radiance changes associated with cloudiness, particularly the temporal changes caused by the appearance or disappearance of clouds, are assumed to be larger than the variability associated with clear conditions. A secondary premise is that the effect of clouds on the radiances is to decrease IR values and/or increase VIS values. The detection algorithm compares the results of a series of tests over several spatial and temporal domains since there is no single space or time relationship of IR and VIS radiance variations that identifies clouds for every location, time of day, and season on earth (Rossow and Garder 1993).

The statistics of IR and VIS radiance variations that support the assumptions used in the cloud detection method are illustrated by Rossow and Garder (1993). These results supplement those of several other studies (Reynolds and Vonder Haar 1977; Coakley and Bretherton 1982; Coakley and Baldwin 1984; Desbois and Sèze 1984; Minnis and Harrison 1984; Rossow et al. 1985; Saunders 1986; Sèze and Desbois 1987; Saunders and Kriebel 1988; Rossow et al. 1989b), particularly Sèze and Rossow (1991a,b). Sensitivity studies were also conducted to test the effects of changing the parameters of the radiance contrast tests, the assumed widths of the radiance distributions, and the magnitudes of the radiance thresholds applied to detect clouds. These results show that the regional variability of the test parameters improves the performance of the cloud detection method for a wide variety of circumstances. They confirm that the time contrast test is the most potent, especially in spatially complex situations (cf., Sèze and Desbois 1987). Use of distribution shape tests for the high-IR and low-VIS portions of the radiance distributions, based on the results of Sèze and Rossow (1991a), allows for improved estimation of clear radiance values by reducing contamination by less variable clouds. The sensitivity test results suggest an uncertainty in detected cloud amounts that is no more than about 10% random, with regional biases of no more than 5% (except the polar regions—see section 3c).

b. Radiance data and radiative transfer model

The IR and VIS radiances are the ISCCP stage B3 reduced-resolution radiances (Schiffer and Rossow 1985; Rossow et al. 1987) from imaging radiometers on a suite of weather satellites. To date, data have been obtained from *Meteosat-2, 3, 4,* and *5, GOES-5, 6,* and *7, GMS-1, 2, 3,* and *4,* and *NOAA-7, 8, 9, 10, 11,* and *12* (see Appendix). The original data have been reduced by sampling to time/space intervals of 3 h and 30 km, preserving the original IR field-of-view (FOV) sizes of 4–7 km. The radiances have been normalized to an absolute calibration standard (Rossow et al. 1987; Brest and Rossow 1992; Rossow et al. 1992; Desormeaux et al. 1993). The cloud detection algorithm uses several other datasets to classify locations by surface properties (Rossow and Garder 1993): the Navy/NOAA Sea Ice–Cover Product, the NOAA Snow Cover Product (Dewey 1987), a land–water identification (adapted from Masaki 1976), the National Geophysical Data Center topography dataset, and an adaptation of Matthews's vegetation/land use datasets (Matthews 1983, 1984).

Once clear IR and VIS radiance values are obtained from the space and time contrast tests and radiance statistics, they are compared to a radiative transfer model of a clear atmosphere to retrieve surface temperature and visible reflectance, respectively. Profiles of atmospheric temperature and layer amounts of precipitable water vapor, together with total column ozone abundance, are specified daily from the TIROS Op-

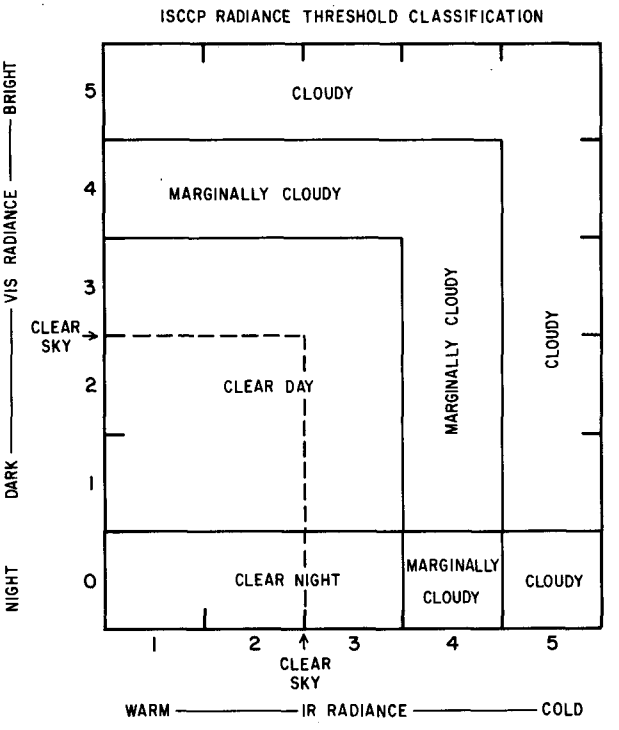

FIG. 2. Schematic of radiance classification of each scene by the radiance threshold tests. Each interval along the axes is equal to the radiance thresholds (Table 1), except for intervals 1 and 5. VIS class = 0 indicates nighttime.

erational Vertical Sounder (TOVS) data products (Kidwell 1991; Smith et al. 1979; McMillin and Dean 1982).

The radiative transfer model for narrowband radiances at the top of a clear atmosphere is essentially the same as described by Rossow et al. (1989b) with the optical constants adjusted to the spectral responses of the *NOAA-7* IR and VIS channels (cf. Rossow et al. 1991). This model calculates radiances as a function of satellite and solar zenith angles and their relative azimuth angle for each image pixel, assumed to be horizontally homogeneous. For IR radiance calculations the atmosphere is represented by nine absorbing gas layers over a blackbody surface. The layer-mean temperatures are specified from TOVS, but interpolated in pressure so as to produce a linear variation of the Planck function within the layer (cf. Lacis and Oinas 1990). Precipitable water amounts from TOVS (and other specified gaseous absorbers with constant abundance) are distributed in each layer with a constant mixing ratio. The treatment of temperature-dependent water vapor absorption has been changed from Rossow et al. (1989b) to include weak line absorption [line strengths from Rothman et al. (1983)], in addition to the continuum absorption [formulation of Roberts et al. (1976)]. Surface temperatures are retrieved assuming a surface emissivity of unity; hence, these values underestimate the true physical temperature of the surface (cf. Rossow et al. 1989b). For VIS radiance calculations the atmosphere is represented by two gas layers over an isotropically scattering surface. The ozone column abundance in the top absorbing layer is from TOVS and the absorption is calculated following Lacis and Hansen (1974) using absorption strengths from Inn and Tanaka (1953). Rayleigh scattering in the second layer is calculated following Lacis and Hansen (1974) for a surface pressure of 1000 mb; topographic effects are neglected. Treating the surface as an isotropic reflector in the retrieval produces an error in the calculated multiply scattered radiation; but since most surfaces are dark, the error is small. For brighter snow and ice surfaces, the reflectivities are more nearly isotropic (Warren 1982).

c. *Validation datasets*

Several datasets are compared with ISCCP surface properties to verify the accuracy of the clear IR and VIS radiances.

The ISCCP sea surface temperatures (SST) represent the temperature of the water surface "skin" (upper millimeter), whereas most other SST datasets represent subsurface water temperatures or mixed-layer bulk temperatures. The primary SST dataset used in the comparison is the Blended Analysis (Reynolds 1988; see also Shea et al. 1992), which combines the NOAA Multi-Channel SST (MCSST) retrieval from AVHRR data (McClain et al. 1985) with ship and buoy measurements to produce monthly mean maps on a 2° grid. The analysis method produces some spatial smoothing so that the actual effective resolution of these data is approximately 6° (Shea et al. 1992). The analysis also changes the AVHRR skin temperatures to agree with the ship/buoy subsurface temperatures. The Blended Analysis data cover the time period from 1982 onward; we performed comparisons for July 1983–December 1987. We also have some daily samples of the MCSST results at 18-km resolution for several months (provided by O. Brown at University of Miami). This analysis has been tuned to agree with buoy subsurface (1-m depth) temperatures. The Comprehensive Ocean–Atmosphere Data Set (COADS) contains ship and buoy measurements of water temperatures below the surface; data from July 1983 to October 1984 are used. Another independent estimate of SST is obtained from microwave radiances measured by the SMMR on *Nimbus-7* (Gloersen et al. 1984); data from October 1983 to October 1984 are used. We also refer to a comparison of ISCCP retrievals of sea ice surface temperatures with available climatologies in the Arctic by Schweiger and Key (1992).

The ISCCP land surface temperatures are also skin temperatures; however, the only available datasets for comparison are near-surface (1–2-m height) air temperatures reported by surface weather observers. We use two versions of this information, direct surface station reports (3-h time intervals) from the U.S. National Meteorological Center collection at NOAA in Asheville, Tennessee, and the twice-daily U.S. Air Force analysis of these same data reported in the *Nimbus-7* cloud climatology dataset (Stowe et al. 1988).

There are few comprehensive surface visible reflectance datasets available. Comparisons are made to an ocean reflectivity dataset (Minnis and Harrison 1984) and to a survey of sea ice albedos by Robinson et al. (1992). The Minnis and Harrison dataset reports top-of-atmosphere visible reflectivities as a function of satellite and solar zenith angles from which we have removed Rayleigh scattering and ozone absorption to infer surface reflectivities.

3. Cloud detection validation

a. *Surface temperature comparisons*

1) SEA SURFACE TEMPERATURES (SST)

Sources of uncertainty in the ISCCP SST values are 1) satellite radiometer calibration, 2) the coefficient for the water vapor continuum absorption, 3) vertical profiles of atmospheric temperature and water vapor abundance, and 4) cloud contamination of the radiances. Only the last source causes an error in cloud detection, since it is the only one that alters the value of clear-sky radiances at the top of the atmosphere. Cloud contamination of the clear-sky radiance values will cause an underestimate of cloud amount (except

possibly in the polar regions where clouds may be warmer than clear conditions in some cases). The remaining sources serve only to increase the disagreement between the ISCCP retrievals and other measurements of SST (Rossow et al. 1989a); hence, a comparison of the ISCCP SST values with other measurements provides an upper limit on the error in the clear IR radiances.

Figure 3 shows the distribution of differences between maps of monthly mean SST from the Blended Analysis (Reynolds 1988) and retrieved from the IR clear-sky composite radiances for 2.5° regions between 60°S and 60°N for 1984–1987. Coastal and sea ice–covered locations have been excluded. Taken at face value, this figure shows that the clear IR radiances, in a global and annual sense, are unbiased and that the uncertainty in their values, as indicated by the value of the standard deviation, is less than the threshold value used for cloud detection (Table 1). The standard deviations of differences between ISCCP and the other SST datasets are also about 2 K; standard deviations of differences among the other SST datasets are between 1 and 2 K. Limited examination of daily and weekly mean SST values from ISCCP and the MCSST show similar results. We also find good agreement between the magnitudes of the diurnal SST variations inferred from the ISCCP analysis ($\approx$1 K) and from other studies (Minnett 1991). We find larger diurnal amplitudes in specific areas in specific seasons; for example, we infer a diurnal SST variation in the Mediterranean in spring/summer of almost 2 K (Bohm et al. 1991). Since some of the difference shown is caused by errors in the Blended Analysis,[1] which are estimated to be about 0.8 K (Reynolds 1988), the uncertainty in the ISCCP SST is <2 K. With the first three sources of error excluded, the implied uncertainty in the clear IR radiances is certainly <2 K for monthly mean values. The regional and seasonal situation is more complicated, so we briefly discuss the first three error sources to isolate the actual detection errors.

The ISCCP SST values in Fig. 3 are brightness temperatures (emissivity assumed to be unity); hence they underestimate physical temperatures by about 0.3–0.7 K [the emissivity of water is about 0.98–0.99, e.g., Saunders (1970), but the magnitude of the correction is reduced in the tropics by reflection of downwelling radiation]. Ship/buoy data represent measurements of bulk temperature that may be ~0.5 K lower or higher than the satellite measurements of skin temperatures under clear conditions (Robinson et al. 1984; Schluessel et al. 1987; Minnett 1991). Additionally, all of the SST datasets may have bias errors associated with errors in instrument calibrations.

[1] Differences in effective spatial resolution contribute as much as 0.3 K to the standard deviation because the lower-resolution blended dataset smooths high-latitude gradients and near-coastal features (see Shea et al. 1992).

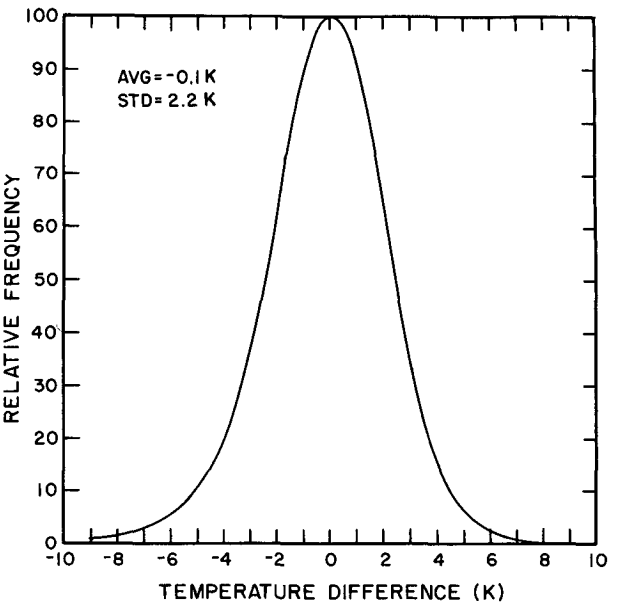

FIG. 3. Frequency distribution of differences between monthly mean values of sea surface temperatures from the blended dataset (Reynolds 1988) and retrieved from ISCCP clear-sky composite IR radiances for 1984–1987 for each 2.5° lat–long region up to 60° latitude in both hemispheres. The average and rms differences in kelvins are indicated.

An estimate of all the bias errors in the ISCCP and blended analysis results can be obtained by comparisons with several other SST datasets that use different sources of information or different analysis methods. Figure 4 shows the global average differences for individual months between several datasets and the ISCCP values. For the period July 1983 through 1987, there are systematic differences of 0.2–1.2 K. Since the trend in differences between the ISCCP and blended datasets is similar to that between ISCCP and COADS, but not between ISCCP and MCSST, we conclude that the trends in Fig. 4 must be relative calibration drifts between satellite and ship values. Two known events are indicated by arrows in the figure. Between January and February 1985, the ISCCP reference AVHRR was changed from that on *NOAA-7* to *NOAA-9*, which apparently produced an increase of ISCCP values by about 0.5 K. Beginning with data for October 1985, an error in the water vapor absorption coefficients used in the earlier ISCCP retrievals was corrected reducing the SST differences by about 0.5 K (Rossow et al. 1991). The overall uncertainty in absolute calibration implied by these comparisons is about ±1 K.

Figure 5 shows the zonal, monthly mean SST differences between the blended and ISCCP values averaged over 1984–1987. The ISCCP values are systematically larger than the blended values by about 1 K over the tropical–subtropical oceans and smaller than the blended values by 2–4 K over middle- to higher-latitude oceans. The differences >4 K poleward of 60°S

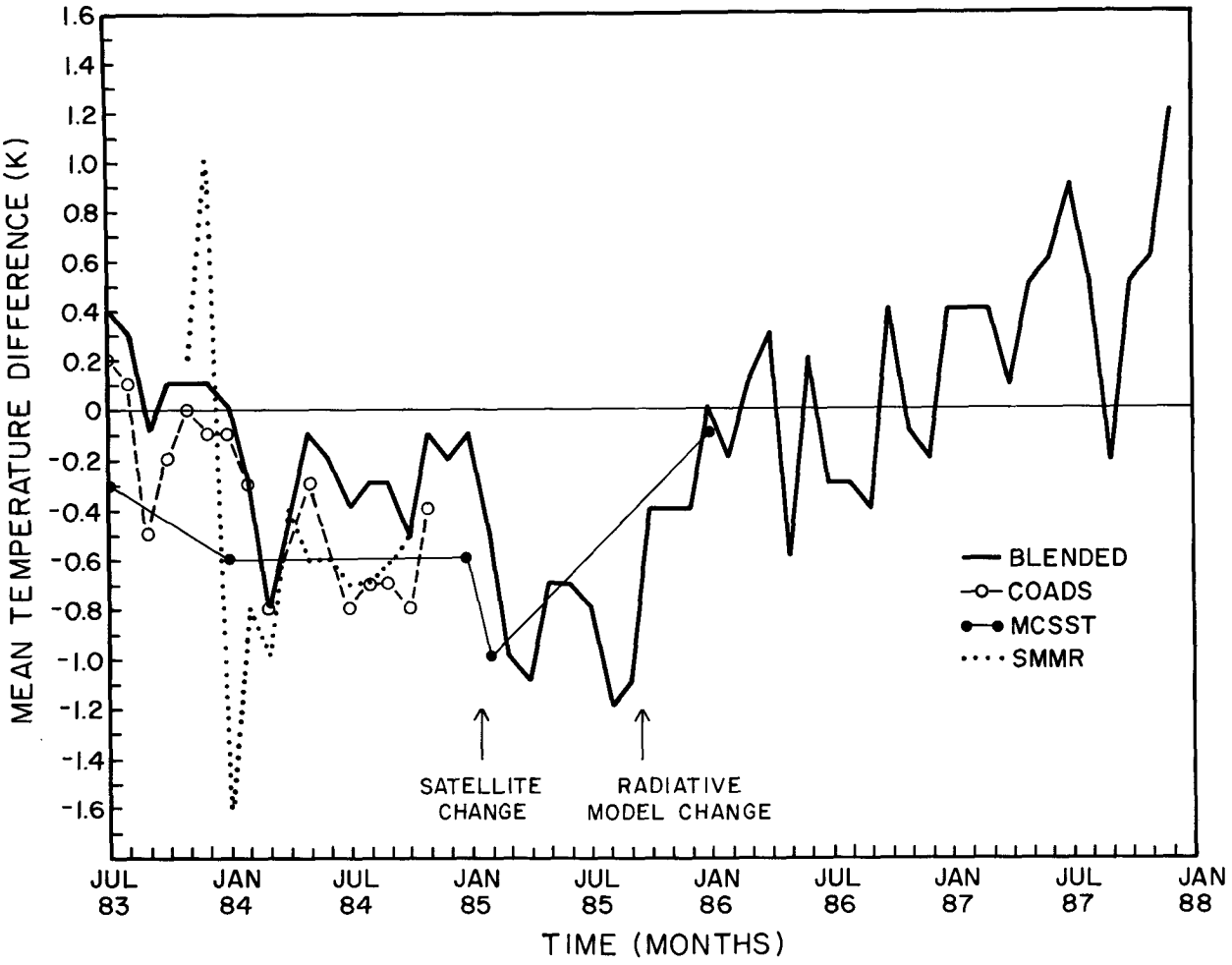

FIG. 4. Variations of the global average differences of monthly mean SST values from each of several datasets and retrieved from ISCCP for each month in 1984–1987. Datasets used are blended SST (Reynolds 1988), COADS (Comprehensive Ocean–Atmosphere Data Set), MCSST (McClain et al. 1985), and SMMR (Gloersen et al. 1984). In early 1985, *NOAA-7* was replaced by *NOAA-9* and in late 1985 the water vapor continuum absorption coefficient was changed in the ISCCP analysis.

and 70°N are caused by different treatments of sea ice: the Blended Analysis assumes a constant value (seawater freezing point) for surface temperature while the ISCCP values are the surface temperature of the ice.

The low-latitude overestimate by ISCCP (negative difference) suggests a problem with water vapor, which would affect the SST retrieval but not cloud detections. This is confirmed by a seasonal shift of the sign of the difference at 30°–50°N from slightly positive in winter to negative in summer. The TOVS atmospheric temperature and humidity data are generally consistent with sonde observations (cf. Oort 1983), with a small underestimate of water vapor amounts (Rossow et al. 1991), which would produce an underestimate of SST.[2] Therefore, the problem must be caused by too much IR absorption by water vapor in the radiative transfer model. An earlier study (Rossow et al. 1989a) suggested too little water vapor absorption, but weak absorption lines have been added to the ISCCP model (Rossow et al. 1991). Use of more recent estimates of the continuum absorption (Barton 1991) would produce a small reduction in ISCCP tropical SSTs by at least 0.5 K. Nevertheless, since clear conditions in the tropics can also be expected to produce the largest differences between skin and bulk temperatures (Schluessel et al. 1987; Minnett 1991), the net bias is still uncertain by about ±0.5 K.

[2] Since the surface temperature is larger than the radiance measured at the top of the atmosphere because of absorption by water vapor, partially offset by some atmospheric emission, smaller water vapor amount causes an underestimate of this difference, which produces a lower retrieved SST.

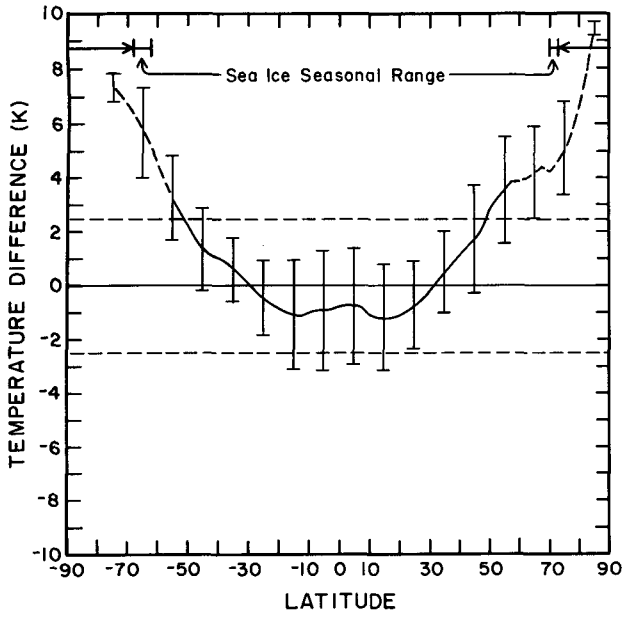

FIG. 5. Zonal mean differences between the monthly mean blended SST and retrieved ISCCP SST values, averaged over 1984–1987. Vertical bars indicate the standard deviation of individual monthly values at each latitude. Arrows indicate the approximate latitudinal extents of sea ice at the seasonal extremes. Dashed lines indicate the ISCCP IR threshold value for reference.

The high IR opacity of the tropical atmosphere (the optical thickness is >0.5 even at 11 μm) amplifies two other sources of error in the ISCCP SST retrievals. Although the noise level for this set of radiometers is generally $\leq$0.5 K for brightness temperatures near 290 K, the retrieval process can amplify this variation to as much as 2 K in the tropics. Moreover, the retrieval is much more sensitive to errors in the TOVS atmospheric temperature and water vapor amounts in the tropics, so that even though the clear-sky composite IR radiance is constant over a 5-day period, erroneous day-to-day variations in the TOVS data can produce day-to-day variations in SST that are too large. This sensitivity can also exaggerate diurnal IR radiance variations into diurnal variations of SST that are too large. None of these effects alters the accuracy of cloud detections.

Some of the higher-latitude difference (reduced by about 0.7 K by the emissivity effect) may be caused by the smoothing in the blended datasets (Shea et al. 1992), particularly near the strong currents. Some of the difference suggests cloud contamination of the clear-sky composite radiances, associated with very persistent cloud cover. The ISCCP annual mean cloud amount over the oceans is already greater than 80% at the latitudes where the SST differences in Fig. 5 are greater than 3 K. A similar problem is apparent in small portions of the marine stratus regions where the ISCCP values of SST are 2–4 K cooler than the blended values. Cloud contamination of the clear IR radiances at higher latitudes is confirmed by several other statistics shown in Fig. 6. The average IR radiance for clear scenes, T_{CLR}, determined using a VIS threshold test, is usually about $\sim$0.5 K colder than the clear-sky composite value of T_{CLR}; but between 45° and 60° latitude in the summer hemispheres the clear scene temperature is larger than the clear-sky composite value (Figs. 6a and 6b). The only other locations where this reversal occurs are in small areas in the marine stratus regimes. At these same locations, the difference between the T_{CLR} values determined with and without the VIS threshold test also increases from <1 K to almost 2 K. The type of clouds contaminating the composite T_{CLR} are not only low level (temperature similar to surface temperature) but very optically thin (probably broken), as indicated by the difference between clear VIS radiances obtained with and without the VIS threshold test (Figs. 6a and 6b). Differences in cloud amounts detected with and without the VIS threshold test, as well as marginal cloud amounts, are both larger in these same locations (not shown). Using the marginal cloud amount to estimate the sensitivity of total cloud amount to changes in the threshold or clear radiances suggests that an underestimate of SST by 1 K would cause an underestimate of cloud amounts at high latitudes of about 5%, averaged over a month. Somewhat larger errors can occur for individual cases.

Figures 6a and 6b also show a decrease of the clear IR radiances for individual scenes relative to the clear-sky composite values at very high latitudes over oceans, yet the clear-sky composite SST values are significantly colder than the blended SST at these latitudes (Fig. 5). Whereas the VIS threshold detects some cloudiness missed by the IR threshold because of cloud contamination in the clear-sky composite IR radiances, as discussed above, this high-latitude behavior and the corresponding convergence of the R_{CLR} values determined with and without the VIS threshold indicate that the VIS radiance threshold is becoming less effective as solar zenith angles increase rapidly toward the poles. At polar latitudes, the 3% VIS radiance threshold is equivalent to 6%–12% VIS reflectance threshold. The 1–2 K differences in T_{CLR} values (Figs. 6a and 6b) suggest an underestimate of monthly mean cloud amount by 5%–10% at very high latitudes.

2) LAND SURFACE TEMPERATURE

Comparison of satellite-measured surface brightness temperatures, T_S, with conventional surface temperature data on land is made much more difficult by a number of factors (cf. Rossow et al. 1989a). The two most important ones are that the land emissivity is much more variable with location and time, because of the effects of vegetation and changing soil moisture content, and that the conventional measurement is of near-surface air temperature, rather than of the temperature of the solid surface or vegetation canopy.

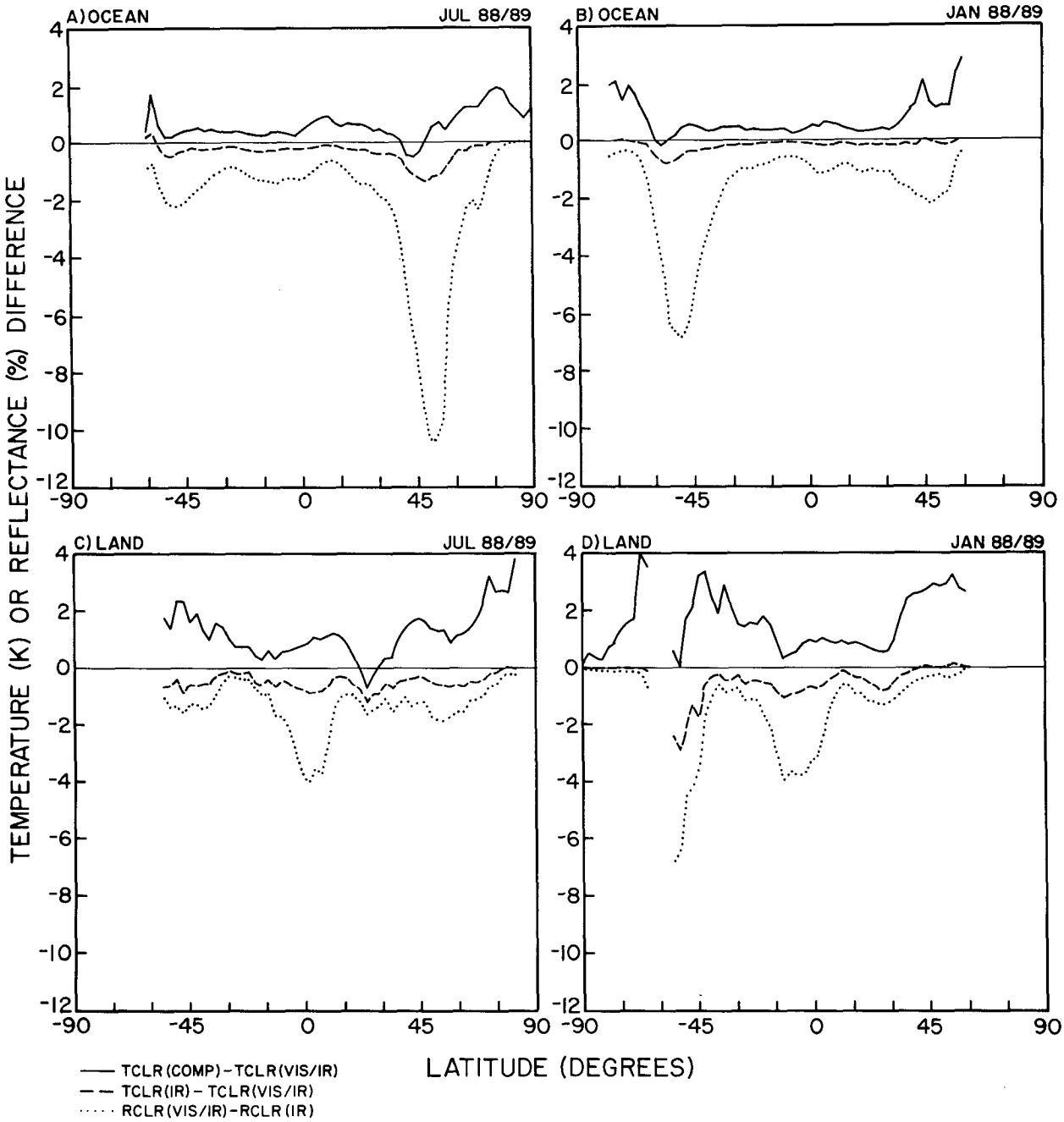

FIG. 6. Zonal mean differences in clear radiance values over ocean for (a) July 1988/89 and (b) January 1988/89 and over land for the same two periods (c) and (d), respectively. Solid lines indicate the difference between the IR radiances (brightness temperatures in kelvins) for the clear-sky composite and for scenes determined to be clear by the VIS/IR radiance threshold tests. Dashed lines indicate the clear IR radiance differences between values obtained from the IR threshold test and from the VIS/IR threshold tests. Dotted lines indicate the differences in clear VIS radiances (reflectances in percent) obtained from the VIS/IR threshold tests and from the IR threshold test.

Moreover, since the land surface temperature responds more rapidly to changing solar insolation associated with changes in cloud cover, there will be a clear-sky bias over land: clear T_s values tend to be higher than average in summer and lower than average in winter (Rossow et al. 1989a).

Figure 7 shows the changes with season and time of day of the average differences between the monthly mean ISCCP land surface temperatures and monthly mean USAF analysis of weather station reports of surface air temperature as a function of ISCCP mean cloud amount. Since the intensity of solar heating is the pri-

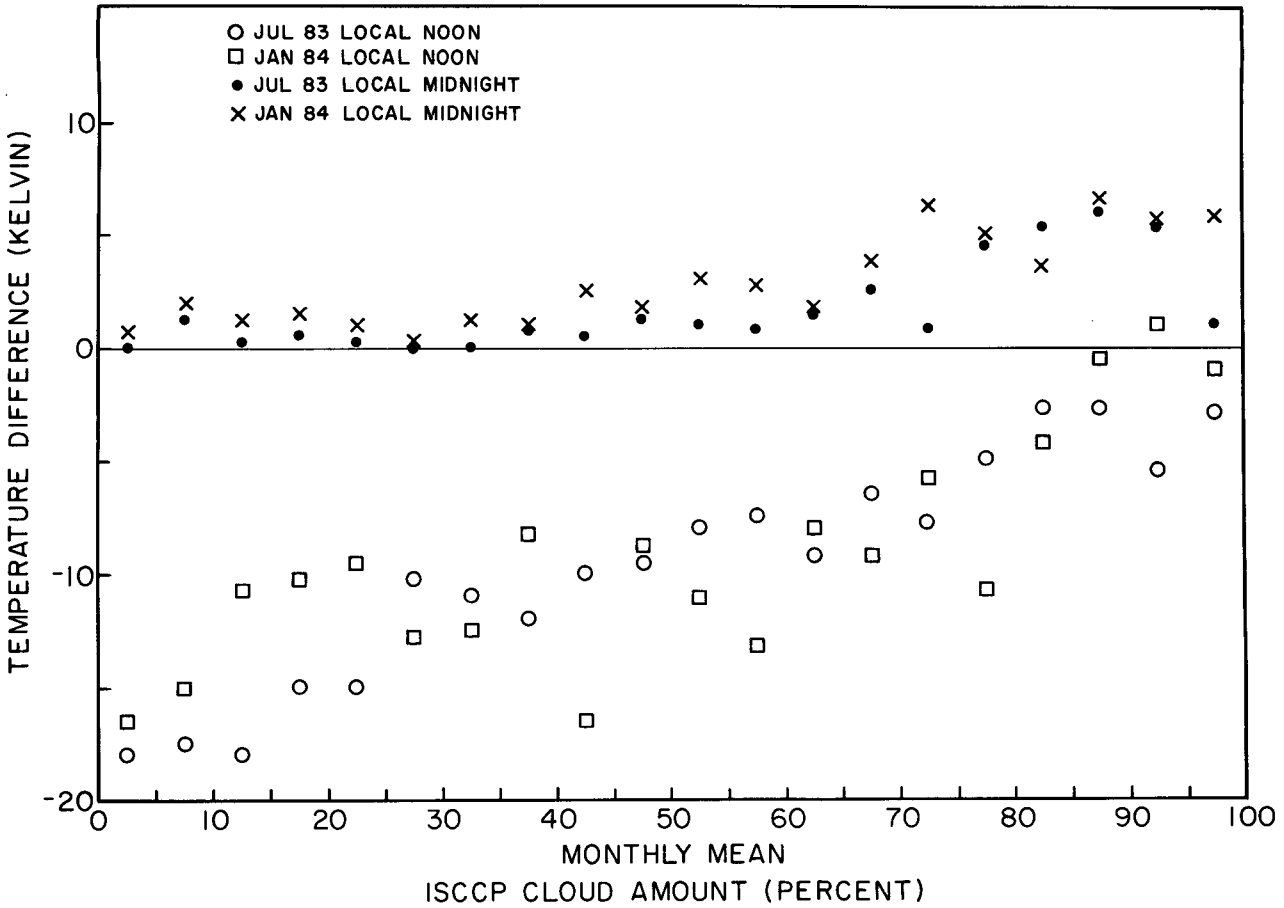

FIG. 7. Mean differences of monthly average land surface temperatures obtained from the USAF analysis of surface weather station observations and retrieved from the ISCCP clear-sky composite IR radiances as a function of monthly mean cloud amount determined by ISCCP. The USAF values represent near-surface air temperatures while the ISCCP values represent surface "skin" brightness temperatures. Results are separated into local noon and midnight times for July 1983 and January 1984 and the comparison performed with ISCCP results averaged to the 4° lat by 5° long grid of the USAF dataset obtained from the *Nimbus-7* cloud climatology dataset (Stowe et al. 1988).

mary cause of differences between the surface skin and air temperatures (cloud effects on radiation cooling at night also play a role), we would expect that the difference between air and skin temperature would be larger in proportion to the amount of sunlight. All the features in Fig. 7 support this expectation: 1) negative differences during the daytime, 2) larger negative differences in daytime with less cloud cover, 3) larger negative differences in summer daytime compared with winter daytime, 4) positive differences at night, 5) smaller positive differences at night with less cloud cover, and 5) little seasonal difference at night. The geographic distribution of these differences [varying amounts of solar heating with latitude and season and varying surface moisture, see Rossow et al. (1989a)] is also consistent with the interpretation that the observed differences in diurnal cycle amplitude between skin and air temperatures do not indicate errors in the satellite analysis (cf. Minnis and Harrison 1984). If the larger differences between air and skin temperature are explained by solar heating, an upper limit on the uncertainty of the ISCCP values can be set by the narrowest difference distribution: for the same dataset shown in Fig. 7, the nighttime difference distributions for both summer and winter have standard deviations of about 4 K.

We argue that separately removing the monthly mean diurnal cycles from the ISCCP and global weather station reports of surface temperatures eliminates most of the radiatively driven differences in these two quantities and isolates the variations associated with weather. Calculating such temperature deviations from the monthly mean diurnal cycle for matched individual surface stations and ISCCP map grid cells (about 280 km in size) and taking differences for individual three-hourly reports over three months (January 1984, July 1985, and October 1986), we obtain the results shown in Fig. 8. The ISCCP values are about 1 K warmer with a standard deviation slightly less than 4 K; the bias varies with season as suggested by Fig. 7.

These differences are larger than errors in the clear radiance because of errors in 1) the ground-based measurements, 2) the water vapor abundances and continuum absorption coefficient used in the satellite analysis, and 3) the geographic variations of emissivity (Rossow et al. 1989a). The first two sources of error may be similar to those over the ocean, ~1 K each, while the latter would bias the ISCCP retrieved temperatures by −(1–2) K, even more over deserts [see discussion and references in Rossow et al. (1989a)]. Since these sources of disagreement affect only the retrieval of a surface temperature from the clear IR radiances, the actual error in clear IR radiances over land is <4 K for individual measurements.

Since the satellite measures surface temperature only under clear conditions, success in capturing a measure of synoptic surface temperature variations in the satellite data depends on the average cloud amount or frequency of clear conditions. Figures 6c and 6d suggest some cloud contamination of clear-sky composite IR radiances in the tropics (especially shown by the larger differences of the R_{CLR} values) where cloud cover can be very persistent. An extreme example occurs at the latitude of the summer monsoon in southern Asia, indicated by the negative difference of T_{CLR} (composite) and T_{CLR} (VIS/IR).

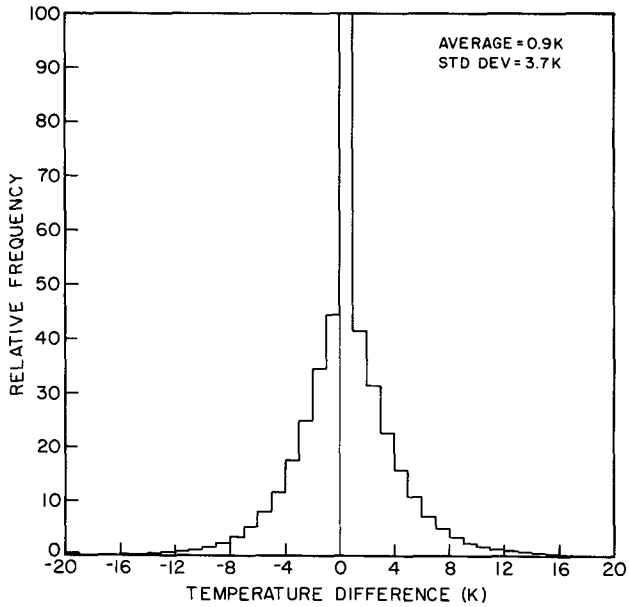

FIG. 8. Frequency distribution of differences between retrieved ISCCP surface skin temperatures (three hourly, averaged over an equal-area grid equivalent to 2.5° resolution at the equator) and individual land surface weather station temperature observations (three hourly), where the respective monthly mean diurnal cycles have been removed from each dataset before comparison. If more than one surface station is present in the ISCCP grid, one value is selected for comparison. Results are for all available surface station reports for January 1984, July 1985, and October 1986 (over 670 000 cases).

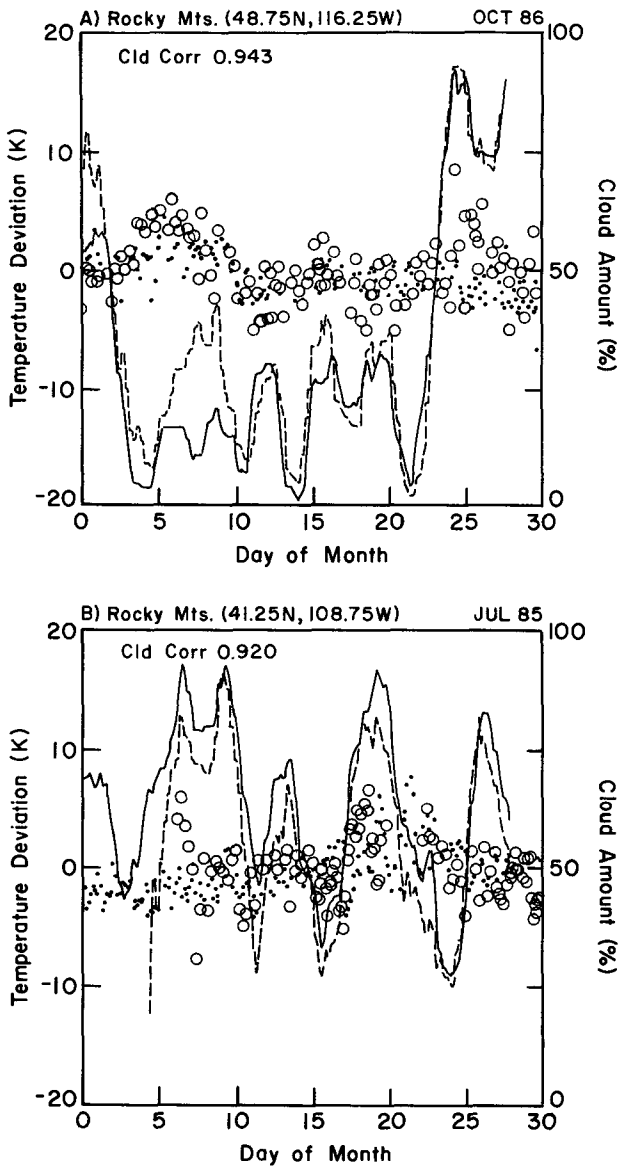

FIG. 9. Comparisons of monthly records of individual cloud amount reports by surface observers (dashed lines) and determinations by the ISCCP analysis (solid lines) and individual surface temperatures obtained by the surface observers (open circles) and determinations by the ISCCP analysis (dots) for two locations in the Rocky Mountains in (a) October 1986 and (b) July 1985. Monthly mean diurnal cycles are separately removed from the two surface temperature records. Observation frequency is every three hours. Correlation of the cloud amount time records is shown as "Cld Corr."

The ISCCP analysis method provides an estimate of the land surface temperature every five days, although in highly cloudy locations this estimate may be based on 15-day statistics. Figure 9 shows a comparison of ISCCP results[3] to cloud amount and surface temper-

[3] Although the clear-sky composite map is constant over 5-day

ature reports from two individual surface stations where the synoptic variations of temperature are small (rms ±2 K), well within the uncertainty attributed to the satellite values. (The temperatures are shown as deviations from monthly mean diurnal cycles.) Both cases show excellent agreement in both temperatures and cloud amounts. Figure 10 shows two other cases where the temperature agreement is even better, yet the cloud amounts are in very poor agreement. The cases in Fig. 9 are both in the Rocky Mountains, where small-scale inhomogeneities could be a problem, though apparently not in these instances, whereas the cases in Fig. 10 are near the coast, where there are large differences in cloud amount between land and water. Such difficulties are familiar and are always present in comparing area-averaged satellite data to pointlike measurements.

The ability of the ISCCP analysis to capture synoptic variations in surface temperature is illustrated in Fig. 11. The first case shows a cooling trend of about 10 K over the month; the ISCCP surface temperatures (diurnal cycle removed) track the surface reports very well and the agreement between the cloud amount values is excellent. In an adjacent location (not shown), the ISCCP results underestimate the temperatures and cloud amounts in the first part of the month. The second case shows a sudden warming of about 7–9 K. Again the ISCCP surface temperatures and cloud amounts track the surface reports very well. These few cases from North America are similar to hundreds of other cases across all continents that we have examined. In section 3c we discuss some cases where the analysis does not work as well.

In general, if errors in cloud detection were caused by errors in surface temperatures, then the differences between satellite and surface measurements of cloud amount and surface temperature would show a correlation of these errors. Table 2 summarizes the comparison of ISCCP results to all surface stations for three months in this form. Only 7% of the cases appear to represent errors in ISCCP cloud detection associated with large errors in the ISCCP surface temperatures (too cold temperature correlated with too low cloud amount and too hot temperature correlated with too high cloud amount). That another 3% of the cases represent a contradictory situation (too cold temperature correlated with too high cloud amount and vice versa) suggests that only about half of these cases are actually cloud detection errors attributable to surface temperature errors. The majority of differences between ISCCP and surface cloud amounts are essentially uncorrelated with surface temperature, suggesting other causes for the differences (cf. Fig. 10).

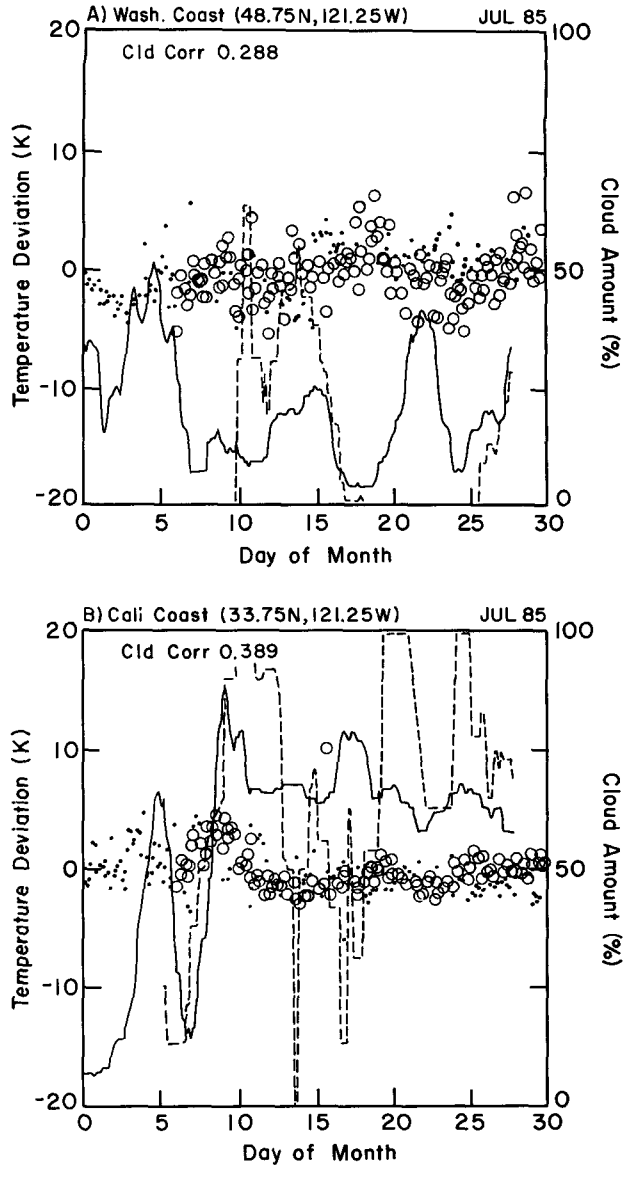

FIG. 10. Same as Fig. 9 for two locations on the west coast of North America in July 1985.

Taken together, Figs. 7–11 and Table 2 suggest that there are no discernible biases in the ISCCP clear IR radiances (surface temperatures), except for some particular locations with large cloud amounts and those associated with the physical difference between air and skin temperatures. Overall, the uncertainties in the clear IR radiances over land are smaller than the thresholds used in the cloud detection algorithm (Table 1). This conclusion implies that the ISCCP monthly mean cloud amounts are underestimated over land by at least 4% (marginal cloud amounts are about 11%,

periods, determined separately for each of eight diurnal phases, the map grid averages of ISCCP surface temperatures shown in Figs. 9, 10, 11, and 15 are calculated only for the particular image pixels present at a particular time. Thus, the small day-to-day variations are caused by day-to-day variations in the spatial coverage of the ISCCP map grid cell. This varying coverage is one source of error in the ISCCP values.

implying a cloud amount sensitivity of about 11%/6 K or about 4%/2 K).

b. Surface reflectance checks

Previous analyses of the time variation of surface visible reflectances by Matthews and Rossow (1987), Rossow et al. (1989a) and, particularly, Sèze and Rossow (1991a) show that time variation is generally not large [as illustrated in Fig. 12 in Rossow and Garder (1993)] and that average surface reflectances are spatially well correlated with their time-minimum values. This general stability in time makes accurate determination of clear visible radiances somewhat simpler

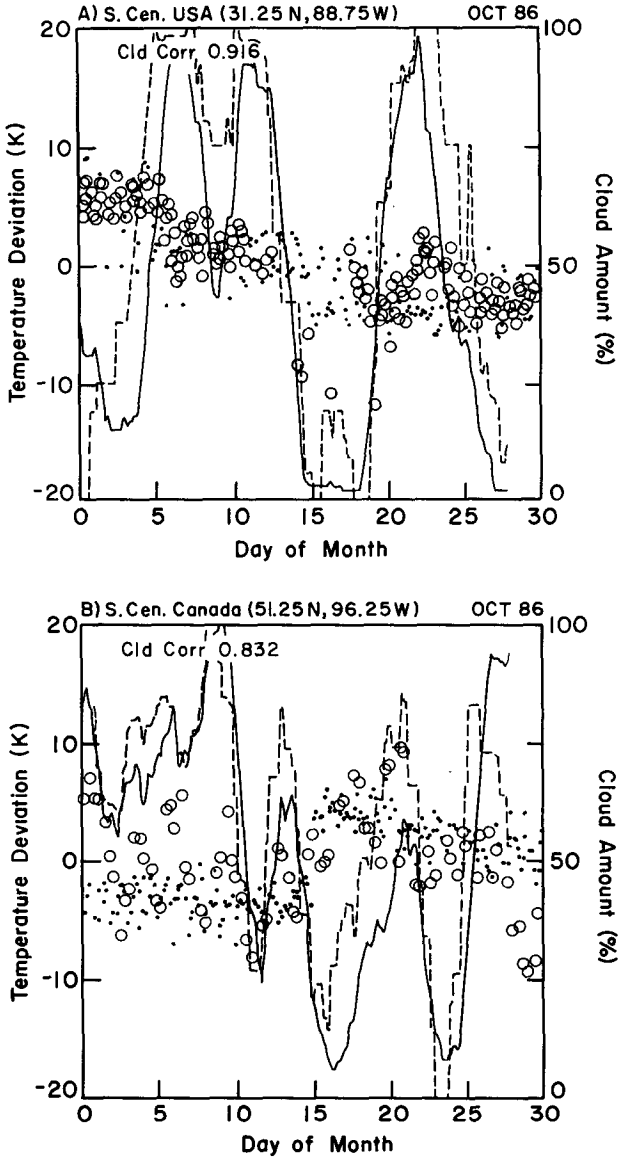

FIG. 11. Same as Fig. 9 for two locations in central North America in October 1986.

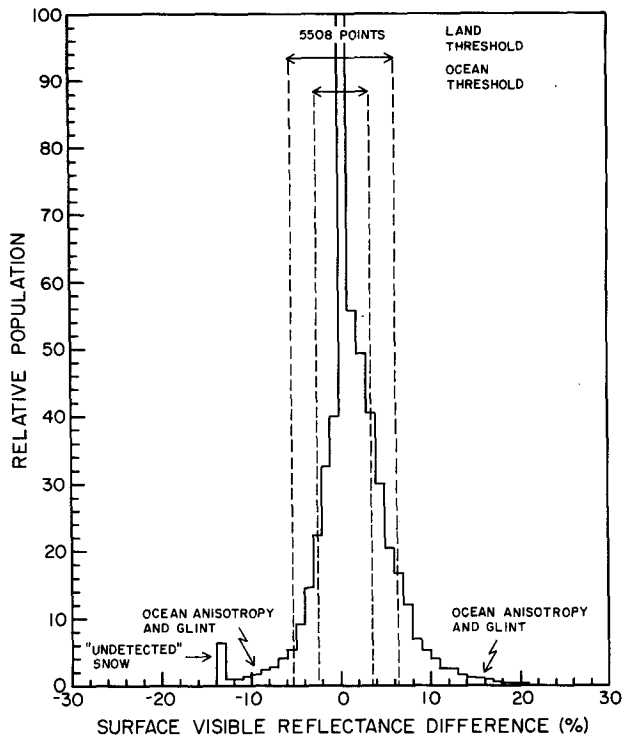

FIG. 12. Frequency distribution of differences in monthly mean, surface visible reflectances for July 1983 and January 1984. Visible radiance thresholds for ocean and land are shown for reference.

than in the infrared. Figure 12 shows the distribution of differences between global monthly mean maps of surface visible reflectance from July 1983 and January 1984 obtained from the ISCCP analysis. The assumed visible radiance thresholds are indicated for comparison. (Note that, on average, the radiance thresholds are larger than the reflectance values indicated because of varying solar illumination.) The large central peak near zero difference is associated with ocean areas, except that the seasonal variation of directional reflectance with solar zenith angle at higher latitudes produces two broad tails (winter hemisphere is brighter than the summer hemisphere). The distribution of values between ±3% and 5% is associated mostly with land areas. The small peak at large negative differences is caused by January snow cover in the Northern Hemisphere. The major problems with accurate determination of clear visible radiances are associated with a few regions of very persistent cloud cover (cf. Figs. 6c and 6d) and the smaller time–space scale variations of the reflectances of snow- and sea ice–covered areas. These problems do not affect large portions of the globe, but are important in those particular regions.

1) OCEAN

Rossow et al. (1989a,b) used a model of ocean visible reflectances as a function of viewing/illumination ge-

TABLE 2. Differences in ISCCP and surface weather station values of cloud amount and surface temperature (monthly mean diurnal temperature cycle removed) for all available stations over the globe for every 3-hour period in January 1984, July 1985, and October 1986 (>670 000 cases). Frequencies of occurrence are shown as a percentage of the total number of cases. ISCCP cloud amount = SATOBS, surface weather report = SURFOBS, ISCCP surface temperature = TS, and surface air temperature = TA.

	TA − TS > 4°C	|TA − TS| ≤ 4°C	TA − TS < −4°C	Total
SATOBS − SURFOBS >7%	1.4	6.3	3.3	11.0
|SATOBS − SURFOBS| ≤7%	12.2	48.5	11.0	71.7
SATOBS − SURFOBS < −7%	3.7	12.0	1.5	17.2
Total	17.3	66.8	15.8	

ometry that agreed with retrieved monthly minimum values to within about 3%, except near glint geometries (cf. Takashima and Takayama 1981). Minnis and Harrison (1984) developed an empirical model of top-of-atmosphere visible reflectances for clear oceans by searching for time minima in GOES visible radiance observations. These two results agree quite well except near glint geometries. We include the search for the monthly minimum visible reflectance in the algorithm, but constrain the resulting values (if no sea ice is present) to agree with the Minnis and Harrison model (corrected to represent surface reflectances) to within 3%. The fact that the monthly minimum values retrieved for the geostationary satellites are rarely corrected illustrates the good correspondence of the model with observations and suggests that the uncertainty in monthly mean values of surface reflectance is $\approx$3%.

There are a few locations where the monthly visible radiance minima are found to be consistently higher than the ocean model: in small portions of the marine stratus regions (off the west coasts of continents in the 15°–35° latitude bands) and in parts of the midlatitude storm tracks, where cloud cover persists for more than one month, and in a few other locations with persistent fogs (such as the North Sea).

In glint geometries the ocean reflectivity varies strongly depending on the nature of surface waves produced by the wind. The Minnis and Harrison model includes a climatological representation of the higher glint reflectivities, however, observed reflectivities are both lower and significantly higher. The ISCCP VIS clear-sky composite is modified to increase the glint reflectivities by as much as 35%; however, we found that the angular distribution varies too strongly with viewing/illumination geometry when compared with observations. Thus, the clear VIS values over ocean for glint geometries are considered unreliable (rms errors ~15%).

2) LAND

Many studies of the variations of land surface visible reflectances have been conducted [see Matthews and Rossow (1987) and Rossow et al. (1989a) for reviews]; the low time variability at 0.6 μm is well established (see also Sèze and Rossow 1991a). Moreover, Brest and Rossow (1992) show that the time stability of the surface reflectances, considered as a global ensemble, is greater than the calibration stability of the radiometers; hence, the final calibration of the visible radiances for ISCCP is adjusted to ensure this global time stability. This method of monitoring calibration has been confirmed by independent information (Brest and Rossow 1992).

The direct use of the monthly minimum reflectance can underestimate the average value because of atmospheric and angular variations that are not accounted for in the analysis, but the high stability of the difference between this value and the modal (or average) value allows for a simple correction. Contamination by very persistent cloudiness still occurs at some locations; this is eliminated in the algorithm by comparing regional values of the monthly minimum reflectances for similar vegetation and surface types. No sufficiently accurate global datasets exist to check the absolute values of the ISCCP surface reflectance values, but they are consistent with published values (cf. Matthews and Rossow 1987). The statistical stability of these values, which are determined for each month of data, ensures that they cause few errors in cloud detection, regardless of their absolute accuracy.

c. Clouds over snow and sea ice

Detection of clouds over snow- and ice-covered surfaces is made more difficult by the significant reduction of contrast between cloud reflectance and temperature and the much higher surface reflectance and lower surface temperature, respectively (Key and Barry 1989; Rossow et al. 1989b). In polar regions, where the solar zenith angle is usually large, differences in scattering between clouds and snow/ice surfaces can produce situations where thinner clouds appear less reflective than clear conditions. Strong temperature inversions are also common, especially in winter (e.g., Serreze et al. 1992), which can lead to cloud temperatures larger than surface temperatures. Cloud detections are also more difficult because the variability of surface properties is somewhat larger, particularly in the marginal zones between snow/ice-covered and snow/ice-free surfaces.

TABLE 3. Comparison of cloud climatologies from the ISCCP C2 dataset (1984–1988), gridded surface weather station reports (SOBS 1971–1981), a manual nephanalysis of METEOR images (1976–1988), and *Nimbus-7* (1980–1984). All cloud amounts are in percent and all differences are with respect to ISCCP amounts. Rms diff values are based on the values in the first four columns; those values shown in parentheses are calculated without *Nimbus-7* values. All results are in an equal-area grid equivalent to 5° lat and 10° long at the equator.

Domain		ISCCP	SOBS	METEOR	*Nimbus-7*	Rms diff
Global	annual	62.6	61.5	60.9	52.9	5.7 (1.4)
	land	47.1	53.3	46.5	45.5	3.7 (4.4)
	ocean	70.2	65.5	67.9	56.5	8.5 (3.7)
	polar	52.3	68.6	50.4	58.0	10.0 (11.6)
	midlatitude	72.2	67.3	68.5	56.9	9.5 (4.3)
	tropical	58.4	55.4	58.2	48.5	6.0 (2.1)
Land	polar	40.5	62.4	37.7	49.6	13.8 (15.6)
	midlatitude	51.4	53.3	49.7	44.4	4.2 (1.8)
	tropical	47.1	49.2	48.4	44.3	2.2 (1.7)
Ocean	polar	65.8	74.9	64.6	67.8	5.4 (6.5)
	midlatitude	81.6	73.7	77.0	62.5	12.2 (6.5)
	tropical	63.0	57.9	62.1	50.3	7.9 (3.7)

These factors affect all observing systems such that very large differences in polar cloud amounts are reported in available climatologies (Table 3, cf. Rossow et al. 1993). The polar regions are also the only parts of the globe where significant differences in the performance statistics of the ISCCP algorithm appear: the number of pixels classified as mixed and marginal in various algorithm tests (cf. Rossow and Garder 1993) and the number of pixels that are much darker/warmer than the clear radiance values are more numerous in the polar regions than anywhere else.

1) SNOW AND SEA ICE VARIATIONS

Rossow et al. (1989a,b) have already shown how well the sea ice- and snow-covered locations can be identified using a simple monthly minimum reflectance approach. Although they tried to reduce the biases associated with the use of minimum reflectances by using the reflectance associated with the maximum temperature, which should be less correlated with the minimum value, the use of month-long time periods to estimate values still led to significant reflectance biases over snow and sea ice–covered areas. In the ISCCP algorithm, we have reverted to the use of the time-minimum reflectance but applied a correction that is approximately the difference between the minimum and the modal value. To avoid the biases caused by time variations of sea ice and snow cover and their age and condition, we use 5-day minimum values for regions identified by other datasets as ice/snow covered.

Comparisons of ISCCP sea ice–visible reflectances with the few available estimates are shown in Table 4. The ISCCP values are brighter than the results from

TABLE 4. Comparison of several sea ice reflectance and broadband albedo estimates. All estimates are uncertain by at least ±5% because the periods and geographic areas used for averaging are not precise. Values from Robinson et al. (1992) are for ice and open water; values marked by * indicate average ice cover < 90%. *NOAA-5* values are corrected only approximately for ozone error (Rossow et al. 1989a).

Location	Time period	ISCCP visible reflectance	Robinson et al. (1992)	*NOAA-5* VIS refl	Other values	References
Central Arctic	spring	0.83	0.80	—	0.80	Curry and Ebert (1992)
	summer	0.70	0.61	0.50	0.52	Scharfen et al. (1987)
	autumn	0.67	—	—	0.60	Curry and Ebert (1992)
Beaufort/Chukchi seas	spring	0.82	0.76 (May)	—	—	Scharfen et al. (1987)
	summer	0.50	0.50*	0.35	0.42	
	autumn	0.45	—	—	—	
East Siberian/Luptev seas	spring	0.75	0.78 (May)	—	—	
	summer	0.50	0.50	0.35	0.40	Scharfen et al. (1987)
	autumn	0.50	—	—	—	
Kara/Barents seas	spring	0.57	0.70 (May)	—	—	
	summer	0.43	0.40*	0.30	0.27	Scharfen et al. (1987)
	autumn	0.30	—	—	—	
Northwest N. Atlantic	spring	0.40	0.71 (May)	—	—	
	summer	0.35	0.52	0.40	0.46	Scharfen et al. (1987)
	autumn	0.25	—	—	—	
Greenland	summer	0.80	—	~0.75	0.75–0.89	Kukla and Robinson (1980)
Antarctica	summer	0.88	—	~0.80	0.82–0.86	Carroll and Fitch (1981)

Rossow et al. (1989a), as expected. The agreement of ISCCP values with the extensive survey by Robinson et al. (1992) is generally very good except for spring values in the Kara/Barents seas and the northwest North Atlantic; but the areal averages in these two regions are sensitive to the fraction of open water included. The apparent errors in surface reflectances of sea ice appear to be no worse than about 10%.

The success of the attempt to capture shorter-term variations in snow reflectances is illustrated by Fig. 13, which shows the distribution of surface visible reflectances obtained from the ISCCP analysis and their week-to-week variations for areas with similar vegetation types, with and without snow cover. The presence of snow is determined by the NOAA snow product, but checked against surface weather station reports in North America. These results show the expected qualitative behavior: the average brightening by snow is somewhat larger (±10%–20%) over grasses, cultivated, and arid locations than over forest and the week-to-week variations are much larger for snow-covered areas, even when they remain snow covered (locations that change from snow covered to snow free or vice versa are excluded from Fig. 13). The arid locations, labeled as snow covered but showing no change in reflectance, are all located in mountainous regions where the low spatial resolution of the snow dataset may cause mislabeling. However, the only effects of the "snow" label on the algorithm are to switch from a 30-day minimum reflectance value (15 days poleward of 50° latitude) to a 5-day minimum for estimation of clear visible radiance and to use a larger visible threshold. Figure 12 in Rossow and Garder (1993) shows that the differences in these different minimum reflectance values are generally small.

Figure 14 shows one case study from among several for winters in North America. Here, a large area undergoes a rapid thaw and snowmelt event. The first two panels compare the surface reflectance patterns and the second two compare the surface temperature patterns in North America inferred from the ISCCP analysis for two dates separated by seven days (the ISCCP clear radiances are constant over 5-day periods). The small circles show all surface weather stations reporting snow cover for the same two days. Also shown as a solid line is the snow cover margin from the snow cover dataset used in the ISCCP analysis, which changes every seven days. The contours of surface reflectance parallel the snow margin used in the analysis with one exception, where in the second week there is snow reported by the surface stations in the forested Appalachian Mountains. The small effect of snow on visible reflectances for forests is shown in Fig. 13 (cf. discussion in Rossow et al. 1989a). The pattern of dramatic decreases in visible reflectance is consistent with the reduced number of stations reporting snow cover. These changes are also associated with a significant warming of surface temperatures. Note that the freezing tem-

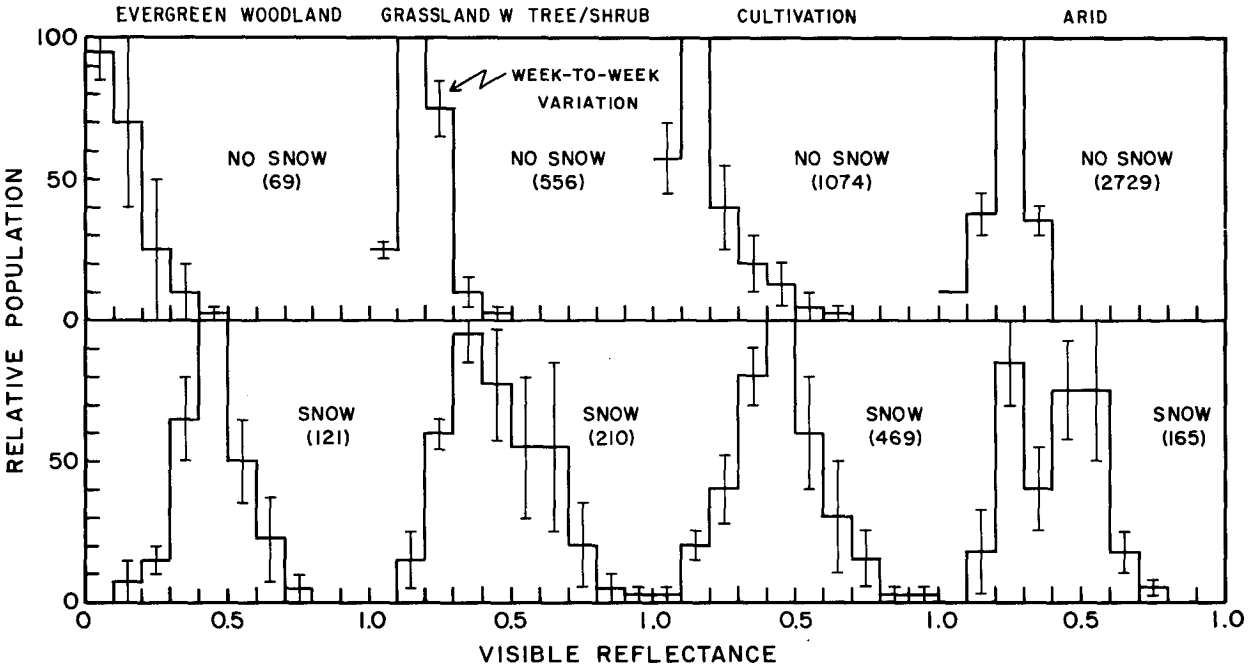

FIG. 13. Frequency distribution of differences in weekly mean, surface visible reflectances in January 1984 for land areas with different vegetation, with and without snow cover. Solid lines indicate the average frequency over the whole month and the vertical bars indicate the standard deviations of individual weekly frequencies. Numbers in parentheses indicate the number of map grid cells included in each category.

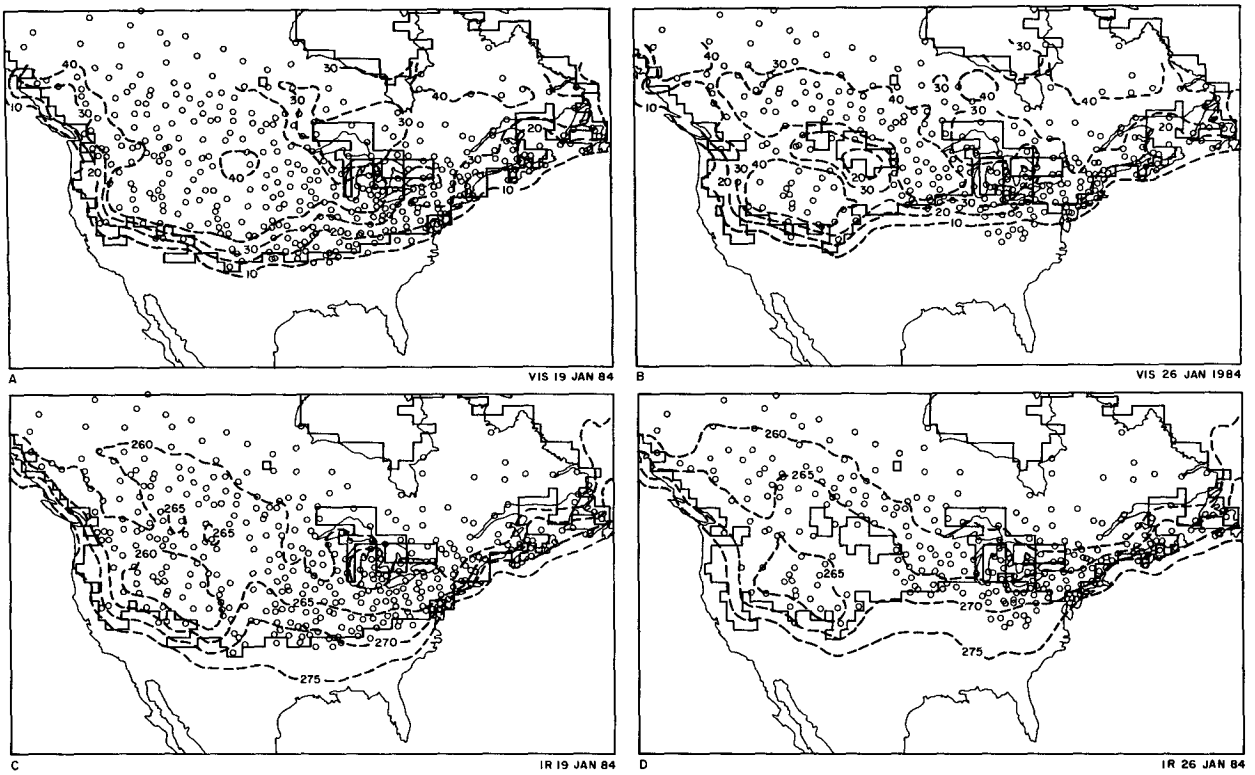

FIG. 14. Distribution of surface weather stations reporting snow cover (open circles) in North America compared with the surface properties inferred from the ISCCP clear-sky composite radiances: (a) visible reflectances on 19 January 1984, (b) visible reflectances on 26 January 1984, (c) surface temperatures on 19 January, and (d) surface temperatures on 26 January. The snow line obtained from the NOAA Snow Product and used in the ISCCP analysis is indicated by the solid (rectangular) contour.

perature contour (brightness temperatures between 265 and 270 K correspond to freezing, depending on the surface emissivity) also parallels the position of the snow margin.

Figure 15 shows more detailed comparisons of the ISCCP and surface observations at four locations in North America during January 1984 (we find many similar cases in Europe and Asia). The first two cases are mountain locations and the second two are in the central plains. The first case in Wyoming (Fig. 15a) shows excellent agreement in both the surface temperature values (mean diurnal cycles removed) and the cloud amounts: the rapid cooling from about 8 to 18 January and the thaw from about 20 to 28 January are readily apparent. In the second case in British Columbia (Fig. 15b), the ISCCP results indicate the qualitative surface temperature changes but underestimate their magnitude by almost 10 K. Early in the month, the ISCCP cloud amounts appear too low, which may be caused by the underestimate of surface temperatures. However, this cold-air outbreak is associated with high cloud amounts that are properly detected (though underestimated) by the ISCCP analysis despite large errors in surface temperature. The third case in Oklahoma (Fig. 15c) has similar temperature errors but smaller under- and overestimates in cloud amount that are correlated with under- and overestimates of surface temperature.

The fourth case in Kansas (Fig. 15d) shows another case like the Oklahoma case, but with much larger cloud amount errors including a significant false detection (from the IR threshold test) during the rapid cooling period. Inspection of the satellite images for several other cases, like that in Fig. 15d where an apparently false cloud detection has occurred, shows that the surface observers sometimes fail to report extensive cirrus overcasts. In other cases, the ISCCP detection is clearly in error, but the error is limited to regions with strong spatial temperature gradients or rapid time changes of temperature. Averaged over the area of the cold-air outbreak, the cloud amount is overestimated only by 15%–20%. Usually, the ISCCP analysis returns to accurate results 1 to 2 days after the rapid cooling event occurs. Monthly mean cloud amounts are less affected by these errors because these events are not frequent and do not involve large areas: all such cases are included in Fig. 8. Since the ISCCP analysis obtains a good estimate of the monthly mean surface temperatures, but underestimates their variability, some cancellation of cloud amount errors also occurs in the

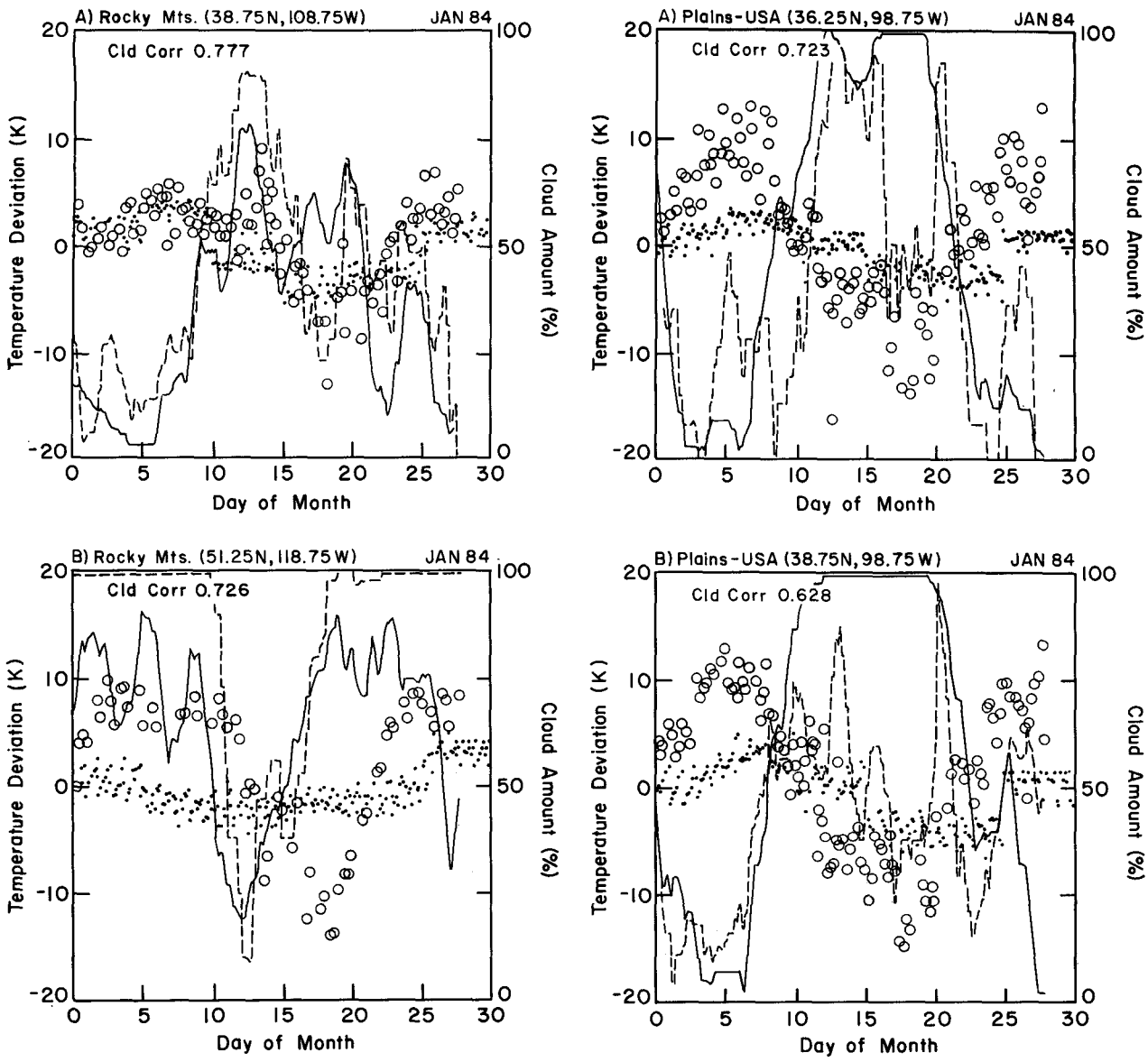

FIG. 15. Same as Fig. 9 for two locations in the Rocky Mountains in January 1984 (a), (b) and for two locations in the U.S. central plains in January 1984 (c), (d).

monthly mean (cf. Table 2). Moreover, these events are often, but not always, associated with large cloud amounts that are detected despite the temperature errors. After examination of such results for three seasons (summer, fall, winter) over all land areas, we conclude that the cases presented in Fig. 15 are examples of the worst problems that are encountered (outside the polar regions).

2) ARCTIC

Compared with surface observations (Warren et al. 1986, 1988), the ISCCP cloud amounts averaged over 60°–90°N are similar in winter and about 25% lower in summer (see Rossow et al. 1993). The ISCCP winter results, however, comprise lower cloud amounts over land areas surrounding the Arctic Ocean and higher cloud amounts over the sea ice relative to surface observations. The surface observations (Warren et al. 1986, 1988) indicate larger winter cloud amounts at lower latitudes, where some sunlit observations are available, but show a sharp decline into the central Arctic, opposite to their summer results. Recent analyses have suggested significant upward revisions of the surface-observed cloud amounts for the winter season because the nighttime observations of surface observers are unreliable (Hahn et al. 1993). Curry and Ebert

(1992) also argue for the inclusion in total cloud amounts of "diamond dust," a form of ice precipitation that occurs mostly in winter, but is not counted as cloud by surface observers, even though its optical thickness may be significant [Curry et al. (1990) report aircraft measurements indicating optical thicknesses >5]. Their estimates suggest that the actual seasonal variation of cloud amount in the central Arctic may be much smaller than previously estimated and that the central Arctic is cloudier than the surrounding land areas year round.

Our retrieved seasonal cycle of surface temperature agrees with that reconstructed by Curry and Ebert (1992), but shows slightly warmer surface temperatures in winter. Schweiger and Key (1992) also confirm good agreement of the ISCCP surface temperatures with buoy and climatological data, but suggest that the observed surface temperature contrast between cloudy and clear conditions may make our values too high by as much as 5 K. Even if actual surface temperatures are warmer in cloudy conditions than in clear conditions, the clouds block the satellite view, unless their optical thickness is ≤ 1. All that matters for proper cloud detection is that the inferred clear-sky temperatures are warmer than the temperatures of actual clouds and about equal to the surface temperatures when it is actually clear. The problem is the occurrence of cloud layers in the persistent temperature inversion (cf. Curry and Herman 1985) that may raise the inferred clear-sky values enough to cause mistaken identification of clear conditions as cloudy. Since the marginally cloudy[4] amount (see Rossow and Garder 1993) is almost 20% in the central Arctic, a 5 K error in the clear radiances might explain the winter cloud amount differences with the surface observations; but the closer agreement of our temperatures with other data does not support this idea entirely. Schweiger and Key also argue that the diamond dust does not affect the radiances enough for detection, but they assume optical thickness values 3–10 times smaller than reported by Curry et al. (1990). Given the large disagreement of surface-based estimates (cf. Hughes 1984) and the general underestimate of cloud amounts at nighttime (Hahn et al. 1993), the accuracy of the large wintertime ISCCP cloud amount in the central Arctic cannot be confirmed.

In summer the ISCCP cloud amounts are much lower than estimated from surface observations and show a decline toward the pole that does not appear in surface data. Note, however, that the number of surface observations actually located in the central Arctic is extremely small. If summer clouds are frequently low level as reported (Huschke 1969; Curry and Herman 1985; Warren et al. 1988; Curry and Ebert 1992), then the ISCCP analysis may not be sensitive enough to detect all of them.

New information about polar clouds can be obtained from the 3.7-μm channel (number 3) on the AVHRR flown on the NOAA polar orbiters (Key and Barry 1989; Raschke et al. 1992; Yamanouchi and Kawaguchi 1992). Radiation at this wavelength comes from both thermal emission and reflected sunlight during daytime; but since the sea ice and snow albedo at this wavelength are significantly lower than at 0.65 μm, there is more contrast between cloudy and clear conditions than at 0.65 μm. Figure 16 shows a sample distribution of 3.7-μm solar radiances[5] separated by the ISCCP cloud algorithm into cloudy (dashed contours) and clear (solid contours) categories. Values of $(T_3 - T_4)$ above 5 K indicate clouds (Key and Barry 1989; Yamanouchi and Kawaguchi 1992). The horizontal axis shows the difference between the channel 4 brightness temperatures (T_4) and the clear-sky value (T_{4CLR}) obtained from the ISCCP analysis. The vertical dotted lines indicate the IR thresholds (a range is shown because of the regional variability of the threshold magnitudes).

The upper panels show results from ice-free ocean and snow-free land where we expect our cloud detection errors to be small. The shape of the clear contours over ocean indicates little bias in the T_{4CLR} values and a very small (2%) population of clouds ($T_3 - T_4 > 5$ K) with T_4 values nearly identical to T_{4CLR}. This confirms discussion in sections 3a1 and 3b that there is a small amount of cloud contamination over high-latitude ocean areas (note cloud amount is >75% in this case), but that it has little effect on the clear-sky temperatures. The overlapping dashed contours show that the VIS threshold is detecting some of the same low-level cloudiness detected by the channel 3 test; in fact, if the ISCCP test is changed from a VIS radiance to a VIS reflectance threshold, almost all of the cloud detected by the channel 3 test is detected by the VIS test.

Over land we see a suggestion of a 3 K cold bias in the clear-sky temperatures and a distribution of clear pixels with $T_4 < T_{4CLR}$ and $(T_3 - T_4) > 5$ that overlaps similar cloudy pixels detected by the VIS threshold. If our T_{4CLR} value had been a few degrees larger (less cloud contamination) and the IR threshold had been about 4 K, we would detect about 3% more cloudiness in this case. The slight bias and suggestion of an IR threshold that is too large are both consistent with the discussion in section 3a(2). Over both ocean and land, the channel 3 test detects some additional low-level cloudiness missed by the regular ISCCP algorithm.

[4] The marginally cloudy amount is determined in the ISCCP algorithm by counting those image pixels with radiances that differ from the clear radiances (lower IR and/or higher VIS) by more than 1 but less than 2 threshold intervals.

[5] The solar part of the 3.7-μm radiance is given approximately by the difference between the channel 3 and channel 4 brightness temperatures, $T_3 - T_4$, since thermal emission with a wavelength distribution like that of a blackbody has $T_3 = T_4$.

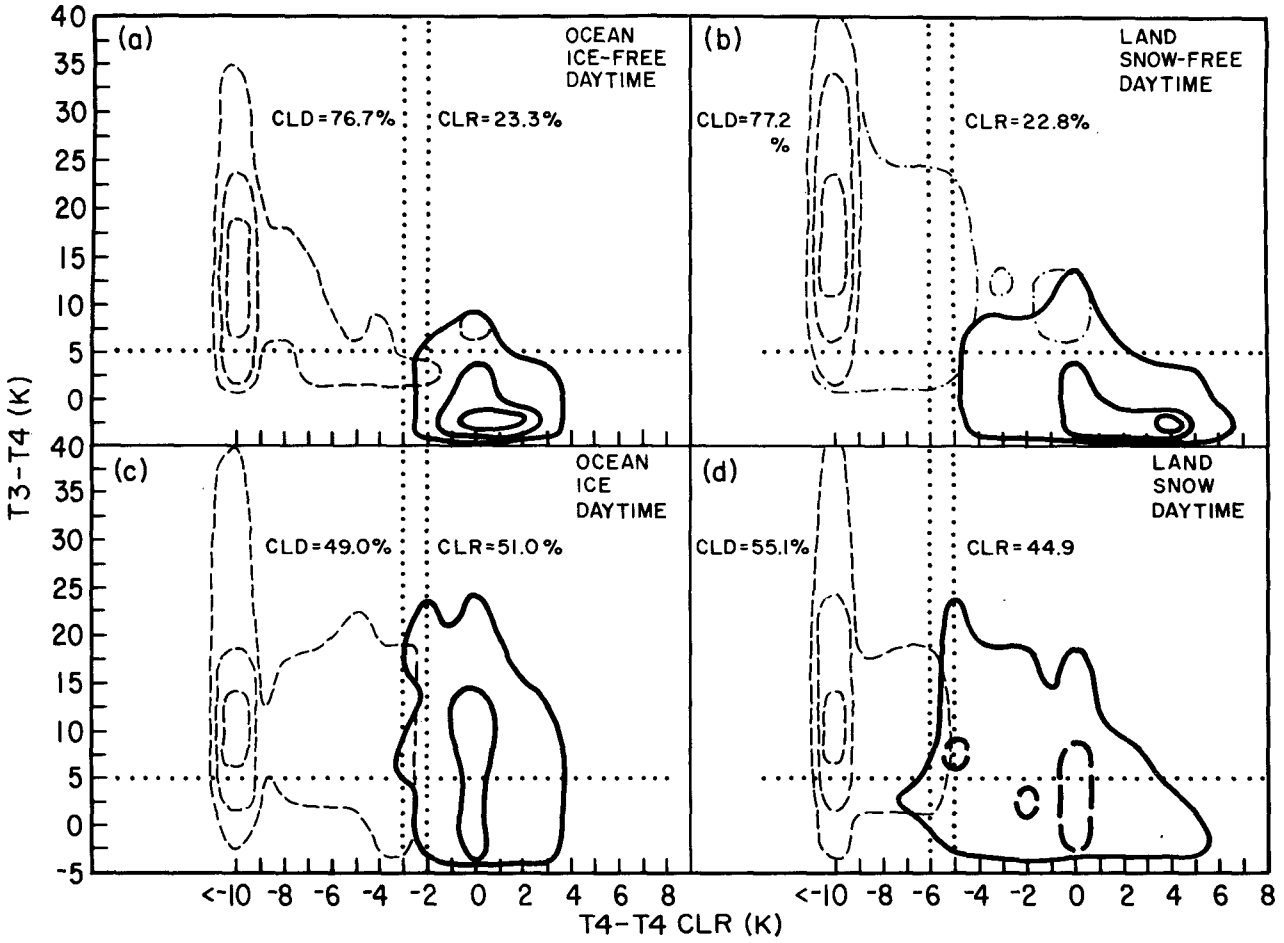

FIG. 16. Frequency distribution of scenes classified by the magnitude of the AVHRR channel 3 (3.7 μm) reflectance, indicated approximately by ($T_3 - T_4$), and by the difference of IR radiance (AVHRR channel 4, T_4), and the clear IR radiance (T_{4CLR}) determined by the ISCCP analysis. Contours indicate fraction of population of cloudy (dashed) and clear (solid) scenes; outermost contour is 1% and the next contours are 5% and 10%. Division into cloudy and clear categories is according to the VIS/IR radiance threshold tests, where the IR threshold is indicated by the vertical dotted lines. The horizontal dotted line is a threshold in ($T_3 - T_4$) similar to that used by Yamanouchi and Kawaguchi (1992). Results are from October 1986 poleward of 50°N.

Note, however, that there is a significant population of pixels in both upper panels that are below the channel 3 threshold, but are definitely clouds with very large contrast in IR, namely, cirrus.

The shape of the contours in the lower panels in Fig. 16 shows a larger population of pixels with T_4 values near T_{4CLR} but with large ($T_3 - T_4$) values than over ice-snow-free surfaces, suggesting that this type of cloudiness occurs especially over ice-snow-covered surfaces. Over sea ice, the shape of the ($T_4 - T_{4CLR}$) contours shows little evidence for a bias in T_{4CLR} and indicates that a smaller IR threshold could not detect these clouds. The very conservative VIS radiance threshold at high latitudes (large solar zenith angles), equivalent to reflectance differences >20%, also does not detect any of these low-level clouds, as indicated by the absence of any overlap of the cloudy and clear contours; a VIS reflectance threshold of 10% is able to detect about 10%–15% more cloud. A channel 3 threshold test would increase the cloud amount by almost 30% for this case, easily accounting for the discrepancy between the ISCCP- and surface-observed cloud amounts over the central Arctic in summer.

The situation over land is much more variable, as shown by the broad distribution of ($T_4 - T_{4CLR}$) values for clear pixels: while there is some hint of a cold bias, most of the cloud contamination, indicated by ($T_3 - T_4 > 5$), is associated with T_4 values that are colder than T_{4CLR}. Decreasing both the VIS and IR thresholds as discussed would increase the cloud amount by 10%–15%, whereas a channel 3 threshold test would increase it by about 24% in this case. About 3% of the extra cloudiness detected by the reduced IR threshold is not detected by either the VIS or channel 3 tests, again indicating the presence of thin cirrus clouds. Such increases in cloud amount over snow-covered land can

account for most of the discrepancy with surface observations.

3) ANTARCTIC

Over sea ice–covered regions near Antarctica, we appear to have less severe cloud detection problems than in the Arctic: cloud amounts larger than those observed from the surface do not appear in the winter. A possible reason for this result is that the combination of much thinner sea ice and a land–ocean geometry that allows more frequent penetration of air masses from the warmer oceans produces both warmer sea ice surface temperatures and less frequent atmospheric temperature inversions. A similar analysis of the 3.7-μm radiances, as shown in Fig. 16, suggests that about 5%–10% more cloudiness is present over the sea ice in summer.

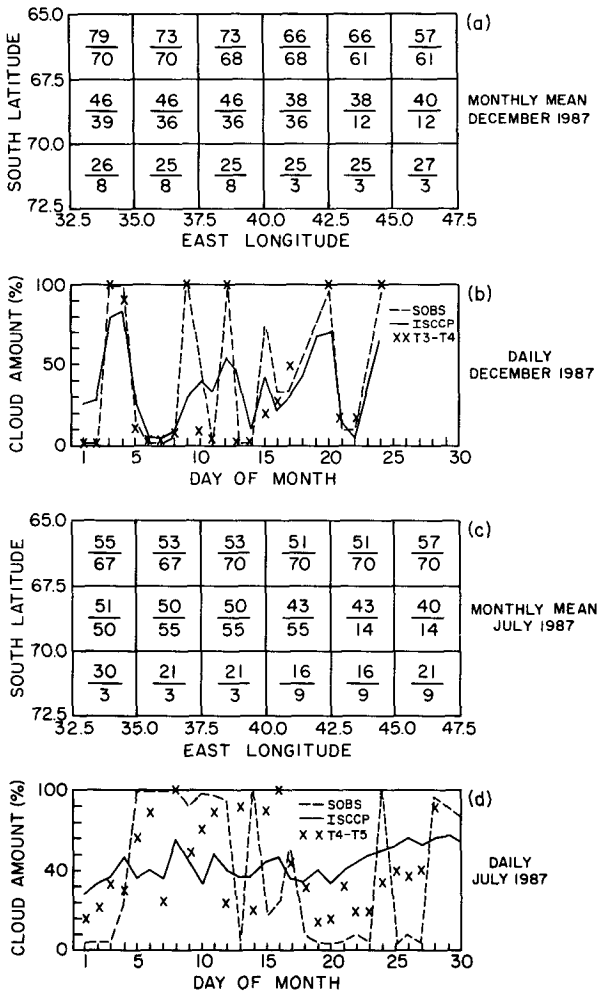

FIG. 17. Comparison of ISCCP cloud amounts for December 1987 and July 1987 to satellite analyses by Yamanouchi and Kawaguchi (1992) and to surface reports from Syowa station in Antarctica. The numbers in the latitude–longitude grid indicate values obtained from AVHRR by Yamanouchi and Kawaguchi (upper) and ISCCP (lower). The line traces show these two satellite results for each day for the map grid containing Syowa station compared to the surface observers estimate of cloud amount (SOBS).

Surface stations in Antarctica are located primarily on the coast, except for the stations near the South Pole. In summer, the South Pole and coastal stations report similar cloud amounts, whereas in winter the South Pole cloud amounts are less than on the coasts (Warren et al. 1986). The ISCCP results show a significant cloud amount gradient between the South Pole and the coastal ocean all year but much larger in summer. The winter surface observation climatology is suspect, however, since the frequency of monthly mean values that are precisely equal to the decadal average value is about five times larger than any other cloud amount value, suggesting the possibility of a large number of bogus reports. Schneider et al. (1989) also find that reported cloud amounts in winter are correlated with lunar brightness (cf. Hahn et al. 1993) and estimate that there is actually little seasonal variation of cloudiness at the South Pole. Most of the extra cloudiness reported by surface observers when the moon is bright appears to be "nonopaque" (Schneider et al. 1989), suggesting that most of the cloudiness missed by the ISCCP analysis (and the surface observers without moonlight) has very low optical thicknesses. Judging from cloud-top temperatures, sometimes $\leq$200 K, inferred from the ISCCP analysis, some of the winter cloudiness may be a thicker version of the springtime polar stratospheric clouds detected by SAGE (Woodbury and McCormick 1986).

Comparison of the ISCCP results with a detailed satellite–surface observer analysis in an area around Syowa station (Yamanouchi and Kawaguchi 1992) shows some agreement in July 1987 (Fig. 17). Their results confirm the magnitude of the near-coastal gradient in the ISCCP cloud amount, decreasing from about 55% over sea ice to about 15%–20% inland (Fig. 17); however, the daily variations of cloud amount reported by the surface observer are larger and show little agreement with either satellite analysis. The agreement between these results and ISCCP is much better in summer, even on a daily basis, but the ISCCP results underestimate inland cloud amounts (Fig. 17). Yamanouchi and Kawaguchi (1992) suggest that use of a threshold test on AVHRR channel 3 reflectances can improve the satellite analysis.

d. Variation of cloud detection with satellite viewing geometry

Examination of the geographic distribution of average ISCCP cloud amounts shows a notable discontinuity in the southern Indian Ocean where there is a gap in coverage by geostationary satellites between Meteosat and GMS (that was to have been filled by data from INSAT). The discontinuity in cloud amounts is associated with the largest change in the

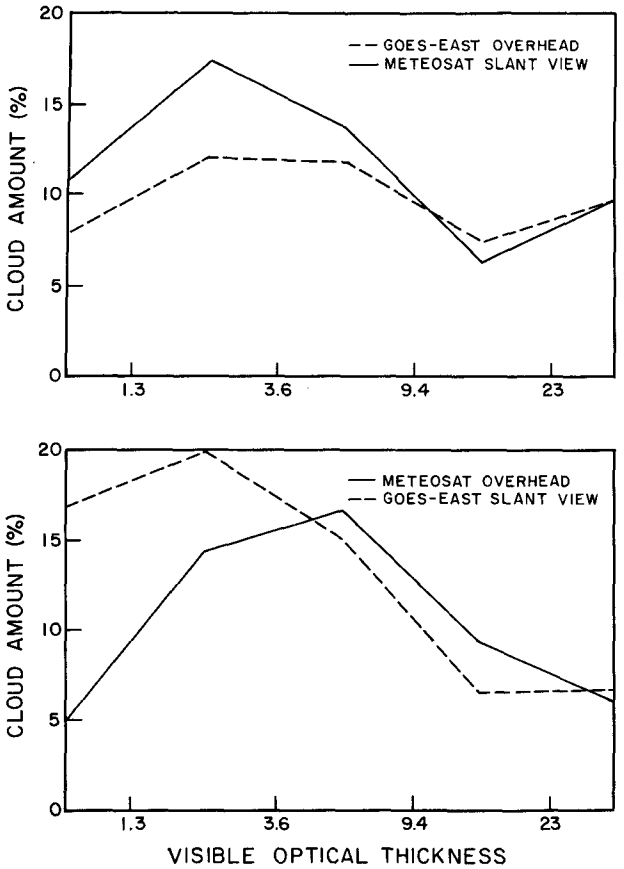

FIG. 18. Variation of cloud amount with optical thickness for two pairs of satellite observations at different viewing zenith angles. In the upper panel, the GOES-East (dashed lines) satellite views each scene from nearly overhead while Meteosat (solid lines) views approximately the same scenes at approximately the same times from a slant angle of over 65°. In the lower panel, Meteosat views from overhead and GOES-East views from the larger slant angle.

average value of the satellite zenith angle of the observations: cloud amounts determined at zenith angles >60° are about 10%–15% larger than those determined at angles <60°. The usual explanation of this variation of cloud amount with viewing zenith angle is that it represents the effect of projecting broken cloud shapes onto a plane perpendicular to the viewing direction (cf. Minnis 1989). Comparison of cloud detections in coincident and collocated[6] observations from two geostationary satellites with very different viewing zenith angles (Fig. 18) suggests an additional reason for this dependence. When a constant radiance difference is used to detect clouds, progressively optically thinner clouds can cause the required radiance difference as the satellite-view slant path increases with increasing viewing zenith angle. Thus, we find that more optically thin clouds are detected at higher zenith angles than at lower values as shown. This effect will be systematic if the atmosphere contains a small population of very thin clouds at most times and locations.

4. Summary and discussion

a. Error estimates

Comparison of surface temperatures and visible reflectances retrieved from clear radiances provides an assessment of the ISCCP cloud detection algorithm applied to infrared and visible radiance images (Table 5). ISCCP sea surface temperatures are generally accurate to within 2 K, with no large biases except for some small areas with persistent overcast in marine stratus and midlatitude storm regimes [section 3a(1)]. Thus, ocean cloud amounts are expected to be accurate to within ±9% (based on marginal cloud amounts) with small (~5%) underestimates in regions of persistent overcast and an ~5% underestimate at night. Land surface temperatures are generally accurate to within 4 K with a cold bias of ~2–3 K over winter land areas [section 3a(2)]. Occasional winter cold-air outbreaks may produce temperature errors approaching 10 K. Thus, land cloud amounts are expected to be accurate to within ±7% but biased low by about 3%–6%. Nighttime cloudiness may be underestimated by about 5%. Surface visible reflectances appear to be accurate to within 3% over oceans, except in areas of ocean glint, and about 3%–5% over land. However, use of a VIS radiance threshold, instead of a VIS reflectance threshold, probably causes a small underestimate of cloud amount at higher latitudes. The ISCCP estimates of snow and sea ice properties and their variations appear to be only slightly less accurate than for other surface types, but there is little data for comparison (section 3c). Surface temperatures appear of similar accuracy as for other ocean and land areas, but may be biased high by a few degrees in polar winters. Surface reflectances appear accurate to within ±10%. Polar regions appear to have unusually large amounts of very low-level cloudiness in summer and very optically thin cloudiness in winter. ISCCP cloud amounts appear to be only slightly lower than other estimates (though higher than many) in polar winter and at least 15%–25% too low in polar summer. There is little evidence for significant false detections except during some cold-air outbreak events over winter land areas.

These estimates represent the accuracy of cloud *detections,* represented as cloud amount, but do not account for possible errors in areal coverage associated with the effects of finite spatial resolution. This issue is considered in a companion paper (Rossow et al. 1993) where a more direct error assessment is obtained

[6] Since these data are samples collected at slightly different times and spatial resolutions and since the positions of the individual image pixels are not constant nor known to better than ±15 km, small differences in these results are expected at all values of optical thickness.

TABLE 5. Summary of bias and [rms] errors of surface temperature (kelvins) and visible reflectances (%) derived from ISCCP clear-sky radiances and the implied bias and [rms] errors in cloud detections expressed as percentage cloud amounts. Rms cloud amount errors are estimated from marginal cloud amounts.

Surface type or region	Surface temperature	Visible reflectance	Cloud error
Open ocean (ice free)	~0 [2]	~0 [3]	~0 [10]
Coastal water	~0 [2]	~0 [3]	−5 [15]
Subtropical marine stratus	−(2–4) [2]	~0 [3]	−(5–10) [20]
High-latitude storm tracks	−(2–3) [3]	+3 [3]	−(5–10) [10]
Ocean glint	—	[>20]	VIS threshold not used
Sea ice	~+2 [4]	~0 [10]	−(20–30) [20]
Land (snow free)	~−1 [4]	~0 [3–5]	−(3–6) [10]
High-latitude land	~−(2–3) [4]	~0 [3–5]	−(6–10) [10]
Snow-/ice-covered land	~−(2–3) [4]	~0 [10]	−(15–25) [15]

by comparison of ISCCP cloud amounts to coincident surface observations and to other cloud climatologies.

b. *Key remaining problems*

The largest remaining problem with cloud detections occurs in the polar regions. Here, the contrast at 0.65 and 11 μm is very low and even reversed at times, preventing detection of a relatively large fraction of the clouds present. This situation may be improved by exploiting other spectral channels on the AVHRR as suggested by a number of authors (e.g., Key and Barry 1989; Raschke et al. 1992; Yamanouchi and Kawaguchi 1992).

The next most significant problem concerns detection of some low-level and thin cirrus cloudiness, particularly over land under winter nighttime conditions, when infrared measurements are the sole source of information. Nighttime detections have been improved using other wavelengths, especially ones far from the Planck peak wavelength (e.g., McClain et al. 1985; d'Entremont 1986); however, such techniques are currently limited by data quality, especially at higher latitudes where the radiances are much lower.

Another problem, highlighted in section 3c, is proper detection of cloudiness over winter land areas during rapid surface temperature changes. Although the errors associated with cold-air outbreaks partially cancel and do not alter monthly cloud amounts too much, they nevertheless make the current results somewhat less useful for study of winter storms. However, each case must be examined separately, since the ISCCP results are not always incorrect.

The last problem is detection of optically thin clouds. If we could go to the limit of infinite sensitivity (perfect information about clear radiances), then cloud amount on earth would always be 100%, since there are some particles in the atmosphere at all times and places. However, at optical thickness values below about 0.3–0.5, we encounter the background tropospheric and stratospheric aerosols that can be confused with thin cirrus and fogs. Indeed, the boundary-layer aerosol includes significant amounts of water (Twomey 1977) so the distinction between "aerosol," "haze," and "cloud" is really based on particle sizes. This becomes a problem both of detection and of discrimination between different particle sizes and compositions, which is beyond any remote sensing capability that we have today. Hence, the practical definition of clouds employed for ISCCP is that they represent those particle populations that produce significant variations in the radiative fluxes, where "significant" represents changes greater than about 3%–6%.

Acknowledgments. This work has benefited from discussions with a large number of colleagues over the years. We wish to thank participants in the algorithm intercomparison studies, particularly A. Arking, J. Coakley, M. Desbois, E. Harrison, P. Minnis, F. Mosher, E. Raschke, E. Ruprecht, G. Sèze, and E. Smith. We wish to highlight the contributions of G. Sèze who worked with us on the crucial final designs; her work on time variations of the radiances was key to use of this concept in the cloud algorithm. We also thank A. Henderson-Sellers, J. Key, R. Saunders, G. Stephens, S. Warren, B. Wielicki, and D. Wylie for discussions of validation. Extensive intercomparisons of ISCCP and other SST datasets were done by J.-H. Wang at Columbia University. ISCCP is the first project of the World Climate Research Programme. During organization and operations of ISCCP, P. Morel was director of the Joint Planning Staff for WCRP at WMO and T. Kaneshige (succeeded by S. Benedict) was the staff member responsible for coordinating ISCCP meetings and reports. The international project manager and source of our funding for ISCCP is Dr. Robert Schiffer (NASA). We thank A. Walker for suggested improvements to the paper. Drafting was done by L. Del Valle and word processing by C. Koizumi; we thank them for their excellent support.

APPENDIX

ISCCP Participants

ISCCP data processing has been accomplished by the combined efforts of several institutions, which are

listed here along with their representatives (in chronological order). The capture of original satellite datasets, quality checking, and their reduction by sampling are performed by the sector processing centers (SPC). For NOAA polar orbiters, the SPC is the National Oceanic and Atmospheric Administration (represented by G. Hunolt, H. Jacobowitz, H. Drahos, J. Gibson, M. Mignono, and K. Kidwell). For Meteosat, the SPC is the European Space Agency (ESA) (R. Saunders, B. Mason). For GOES-East, the SPC was the University of Wisconsin (R. Fox, D. Wylie) and is now the Atmospheric Environment Service (AES) of Canada (S. Woronko, S. Lapczak, F. Bowkett, D. McKay, Y. Durocher). For GOES-West, the SPC is Colorado State University (CSU) (G. G. Campbell). The University of Wisconsin also serves as a backup to AES and CSU and produces special datasets for related research. For GMS, the SPC is the Japan Meteorological Agency (JMA) (A. Kurosaki, I. Kubota, T. Nuomi, K. Shuto). Normalization of geostationary satellite radiances to those measured by the polar orbiters is performed by the Satellite Calibration Center (SCC) at the Centre de Meteorologie Spatiale in France (N. Beriot, G. Therry, Y. Desormeaux). The ISCCP datasets are produced and analyzed at the Global Processing Center at NASA Goddard Institute for Space Studies (processing group led by E. Kinsella and A. Walker). NOAA serves as the International Central Archives (ICA) for ISCCP. In addition to the data center representatives, membership of the JSC Working Group on Data Management for ISCCP (now for all WCRP radiation projects) included T. Vonder Haar and E. Raschke; ex-officio members representing the WCRP are S. Benedict (who succeeded T. Kaneshige) and R. Schiffer (project manager).

REFERENCES

Barton, I. J., 1991: Infrared continuum water vapor absorption coefficients derived from satellite data. *Appl. Optics,* **30,** 2929–2934.

Bohm, E., S. Marullo, and R. Santoleri, 1991: AVHRR visible-IR detection of diurnal warming events in the western Mediterranean Sea. *Int. J. Remote Sens.,* **12,** 695–701.

Brest, C. L., and W. B. Rossow, 1992: Radiometric calibration and monitoring of NOAA AVHRR data for ISCCP. *Int. J. Remote Sens.,* **13,** 235–273.

Carroll, J. J., and B. K. Fitch, 1981: Effects of solar elevation and cloudiness on snow albedo at the South Pole. *J. Geophys. Res.,* **86,** 5271–5276.

Coakley, J. A., and F. P. Bretherton, 1982: Cloud cover from high-resolution scanner data: Detecting and allowing for partially filled fields of view. *J. Geophys. Res.,* **87,** 4917–4932.

——, and D. G. Baldwin, 1984: Towards the objective analysis of clouds from satellite imagery. *J. Climate Appl. Meteor.,* **23,** 1065–1099.

Curry, J. A., and G. F. Herman, 1985: Infrared radiative properties of summertime Arctic stratus clouds. *J. Climate Appl. Meteor.,* **24,** 525–538.

——, and E. E. Ebert, 1992: Annual cycle of radiative fluxes over the Arctic Ocean: Sensitivity to cloud optical properties. *J. Climate,* **5,** 1267–1280.

——, F. G. Meyer, L. F. Radke, C. A. Brock, and E. E. Ebert, 1990: Occurrence and characteristics of lower tropospheric ice crystals in the Arctic. *Int. J. Climatol.,* **10,** 749–764.

d'Entremont, R. P., 1986: Low- and mid-level cloud analysis using nighttime multispectral imagery. *J. Climate Appl. Meteor.,* **25,** 1853–1869.

Desbois, M., and G. Sèze, 1984: Use of space and time sampling to produce representative satellite cloud classification. *Ann. Geophys.,* **2,** 599–606.

Desormeaux, Y., W. B. Rossow, C. L. Brest, and C. G. Campbell, 1993: Normalization and calibration of geostationary satellite radiances for ISCCP. *J. Atmos. Oceanic. Technol.,* **10,** 304–325.

Dewey, K. F., 1987: Satellite-derived maps of snow cover frequency for the Northern Hemisphere. *J. Climate Appl. Meteor.,* **26,** 1210–1229.

Gloersen, P., D. J. Cavalieri, A. T. C. Chang, T. T. Wilheit, W. J. Campbell, O. M. Johannessen, K. B. Katsaros, K. F. Kunzi, D. B. Ross, D. Staelin, E. P. L. Windsor, F. T. Barath, P. Gudmandsen, E. Langham, and R. O. Ramseier, 1984: A summary of results from the first NIMBUS-7 SMMR observations. *J. Geophys. Res.,* **89,** 5335–5344.

Hahn, C. J., S. G. Warren, and J. London, 1993: Use of moonlight data in the determination of nighttime cloudiness from surface observations. *J. Climate,* submitted.

Hughes, 1984: Global cloud climatologies: A historical review. *J. Climate Appl. Meteor.,* **23,** 724–751.

Huschke, R. E., 1969: *Arctic cloud statistics from "air-calibrated" surface weather observations.* Rand Corp., RM-6173-PR, 79 pp.

Inn, E. C. Y., and Y. Tanaka, 1953: Absorption coefficient of ozone in the ultraviolet and visible regions. *J. Opt. Soc. Amer.,* **43,** 870–873.

Key, J., and R. G. Barry, 1989: Cloud cover analysis with Arctic AVHRR data. 1. Cloud detection. *J. Geophys. Res.,* **94,** 8521–8535.

Kidwell, K. B., 1991: *NOAA Polar Orbiter Data Users Guide (TIROS-N, NOAA-6, NOAA-7, NOAA-8, NOAA-9, NOAA-10, NOAA-11 and NOAA-12).* Environmental Data and Information Service, National Oceanic and Atmospheric Administration, U.S. Dept. of Commerce, Washington, D.C. 280 pp.

Kukla, G., and D. Robinson, 1980: Annual cycle of surface albedo. *Mon. Wea. Rev.,* **108,** 56–68.

Lacis, A. A., and J. E. Hansen, 1974: A parameterization for the absorption of solar radiation in the earth's atmosphere. *J. Atmos. Sci.,* **31,** 118–133.

——, and V. Oinas, 1990: A description of the correlated *k*-distribution method for modeling nongrey gaseous absorption, thermal emission, and multiple scattering in vertically inhomogeneous atmospheres. *J. Geophys. Res.,* **96,** 9027–9063.

Masaki, G. T., 1976: The Wolf Plotting and Contouring Package. GSFC Computer Program Lib. #A00227, Computer Sciences Corporation, NASA Goddard Space Flight Center, Greenbelt, MD, 187 pp.

Matthews, E., 1983: Global vegetation and land use: New high resolution data bases for climate studies. *J. Climate Appl. Meteor.,* **22,** 474–487.

——, 1984: Prescription of land-surface boundary conditions in GISS GCM II: A simple method based on high-resolution vegetation data bases. NASA Tech. Memo. #86096. [Available from NASA Goddard Space Flight Center, Greenbelt, MD.]

——, and W. B. Rossow, 1987: Regional and seasonal variations of surface reflectance from satellite observations at 0.6 μm. *J. Climate Appl. Meteor.,* **26,** 170–202.

McClain, E. P., W. G. Pichel, and C. C. Walton, 1985: Comparative performance of AVHRR-based multichannel sea surface temperatures. *J. Geophys. Res.,* **90,** 11 587–11 601.

McMillin, L. M., and C. Dean, 1982: Evaluation of a new operational technique for producing clear radiances. *J. Appl. Meteor.,* **21,** 1005–1014.

Minnett, P. J., 1991: Consequences of sea surface temperature variability on the validation and applications of satellite measurements. *J. Geophys. Res.,* **96,** 18 475–18 489.

Minnis, P., 1989: Viewing zenith angle dependence of cloudiness determined from coincident GOES EAST and GOES WEST data. *J. Geophys. Res.*, **94,** 2303–2320.

——, and E. F. Harrison, 1984: Diurnal variability of regional cloud and clear sky radiative parameters derived from GOES data. Part I: Analysis method. *J. Climate Appl. Meteor.*, **23,** 993–1011.

Oort, A. H., 1983: Global Atmospheric Circulation Statistics, 1958–1973. NOAA Professional Paper 14, NOAA Geophysical Fluid Dynamics Laboratory, U.S. Dept. of Commerce, Rockville, MD, 180 pp.

Raschke, E., P. Bauer, and H. J. Lutz, 1992: Remote sensing of clouds and surface radiation budget over polar regions. *Int. J. Remote Sens.*, **13,** 13–22.

Reynolds, R. W., 1988: A real-time global sea surface temperature analysis. *J. Climate,* **1,** 75–86.

Reynolds, D. W., and T. H. Vonder Haar, 1977: A bi-spectral method for cloud parameter determination. *Mon. Wea. Rev.*, **105,** 446–457.

Roberts, R. E., J. E. A. Selby, and L. M. Biberman, 1976: Infrared continuum absorption by atmospheric water vapor in the 8–12 μm window. *Appl. Opt.*, **15,** 2085–2090.

Robinson, I. S., N. C. Wells, and H. Charnock, 1984: The sea surface thermal boundary layers and its relevance to the measurement of sea surface temperature by airborne and spaceborne radiometers. *Int. J. Remote Sens.*, **5,** 19–46.

Robinson, D. A., M. C. Serreze, R. G. Barry, G. Scharfen, and G. Kukla, 1992: Large-scale patterns and variability of snowmelt and parameterized surface albedo in the Arctic Basin. *J. Climate,* **5,** 1109–1119.

Rossow, W. B., and L. C. Garder, 1993: Cloud detection using satellite measurements of infrared and visible radiances for ISCCP. *J. Climate,* **6,** 2341–2369.

——, F. Mosher, E. Kinsella, A. Arking, M. Desbois, E. Harrison, P. Minnis, E. Ruprecht, G. Seze, C. Simmer, and E. Smith, 1985: ISCCP cloud algorithm intercomparison. *J. Climate App. Meteor.*, **24,** 877–903.

——, E. Kinsella, A. Wolf, and L. Garder, 1987: International Satellite Cloud Climatology Project (ISCCP) Description of Reduced Resolution Radiance Data. WMO/TD No. 58. World Meteorological Organization, 143 pp. [Available from World Meteorological Organization, Geneva, Switzerland.]

——, C. L. Brest, and L. C. Garder, 1989a: Global, seasonal surface variations from satellite radiance measurements. *J. Climate,* **2,** 214–247.

——, L. C. Garder, and A. A. Lacis, 1989b: Global, seasonal cloud variations from satellite radiance measurements. Part I: Sensitivity of analysis. *J. Climate,* **2,** 419–458.

——, L. C. Garder, P. J. Lu, and A. W. Walker, 1991: International Satellite Cloud Climatology Project (ISCCP) Documentation of Cloud Data. WMO/TD-No. 266 (Revised). World Meteorological Organization, Geneva, 76+ pp. [Available from World Meteorological Organization, Geneva, Switzerland.]

——, Y. Desormeaux, C. L. Brest, and A. W. Walker, 1992: International Satellite Cloud Climatology Project (ISCCP) Radiance Calibration Report. WMO/TD-No. 520, WCRP-77. [Available from World Meteorological Organization, Geneva, Switzerland.]

——, A. W. Walker, and L. C. Garder, 1993: Comparison of ISCCP and other cloud amounts. *J. Climate,* **6,** 2394–2418.

Rothman, L. S., R. R. Gamache, A. Barbe, A. Goldman, J. R. Gille, L. R. Brown, R. A. Toth, J. M. Flaud, and C. Camy-Peyret, 1983: AFGL atmospheric absorption line parameters compilation: 1982 edition. *Appl. Opt.*, **22,** 2247–2256.

Saunders, P., 1970: Corrections for airborne radiation thermometry. *J. Geophys. Res.*, **75,** 7596–7601.

Saunders, R. W., 1986: An automated scheme for removal of cloud contamination from AVHRR radiances over western Europe. *Int. J. Remote Sens.*, **7,** 867–886.

——, and Kriebel, 1988: An improved method for detecting clear sky and cloudy radiances from AVHRR data. *Int. J. Remote Sens.*, **9,** 123–150.

Scharfen, G., R. G. Barry, D. A. Robinson, G. Kukla, and M. C. Serreze, 1987: Large-scale patterns of snow melt on Arctic sea ice mapped from meteorological satellite imagery. *Ann. Glacial,* **9,** 1–6.

Schiffer, R. A., and W. B. Rossow, 1983: The International Satellite Cloud Climatology Project (ISCCP): The first project of the World Climate Research Program. *Bull. Amer. Meteor. Soc.*, **64,** 779–784.

——, ——, 1985: ISCCP global radiance data set: A new resource for climate research. *Bull. Amer. Meteor. Soc.*, **66,** 1498–1505.

Schluessel, F., H.-Y. Shin, W. J. Emery, and H. Grassl, 1987: Comparison of satellite-derived sea surface temperatures with in situ measurements. *J. Geophys. Res.*, **92,** 2859–2874.

Schneider, G., P. Paluzzi, and J. P. Oliver, 1989: Systematic error in synoptic sky cover record of the South Pole. *J. Climate,* **2,** 295–302.

Schweiger, A. J., and J. R. Key, 1992: Arctic cloudiness: Comparison of ISCCP-C2 and *Nimbus-7* satellite derived cloud products with a surface-based cloud climatology. *J. Climate,* **5,** 1514–1527.

Serreze, M. C., J. D. Kahl, and R. C. Schnell, 1992: Low-level temperature inversions of the Eurasian Arctic and comparison with Soviet drifting station data. *J. Climate,* **5,** 615–630.

Sèze, G., and M. Desbois, 1987: Cloud cover analysis from satellite imagery using spatial and temporal characteristics of the data. *J. Climate Appl. Meteor.*, **26,** 287–303.

——, and W. B. Rossow, 1991a: Time-cumulated visible and infrared radiance histograms used as descriptors of surface and cloud variations. *Int. J. Remote Sens.*, **12,** 877–920.

——, and ——, 1991b: Effects of satellite data resolution on measuring the space–time variations of surfaces and clouds. *Int. J. Remote Sens.*, **12,** 921–952.

Shea, D. J., K. E. Trenberth, and R. W. Reynolds, 1992: A global monthly sea surface temperature climatology. *J. Climate,* **5,** 987–1001.

Smith, W. L., H. M. Woolf, C. M. Hayden, D. Q. Wark, and L. M. McMillin, 1979: The TIROS-N Operational Vertical Sounder. *Bull. Amer. Meteor. Soc.*, **60,** 117–118.

Stowe, L. L., C. G. Wellemeyer, T. F. Eck, H. Y. M. Yeh, and the *Nimbus-7* Cloud Data Processing Team, 1988: *Nimbus-7* global cloud climatology. Part I: Algorithms and validation. *J. Climate,* **1,** 445–470.

Takashima, T., and Y. Takayama, 1981: Emissivity and reflectance of the model sea surface for use of the AVHRR data of NOAA satellites. *Pap. Meteor. Geophys.*, **32,** 267–274.

Twomey, S., 1977: *Atmospheric Aerosols.* Elsevier Scientific, 302 pp.

Warren, S. G., 1982: Optical properties of snow. *Rev. Geophys. Space Phys.*, **20,** 67–89.

——, C. J. Hahn, J. London, R. M. Chervin, and R. L. Jenne, 1986: Global distribution of total cloud and cloud type amounts over land. NCAR Tech. Note TN-273 + STR/DOE Tech. Rep. ER/60085-H1, 29 pp. + 200 maps. [NTIS number DE87-00-6903]

——, ——, ——, ——, and ——, 1988: Global distribution of total cloud and cloud type amounts over the ocean. NCAR Tech. Note TN-317 + STR/DOE Tech. Rep. ER-0406, 42 pp. + 170 maps. [NTIS number DE90-00-3187]

Woodbury, G. E., and M. P. McCormick, 1986: Zonal and geographic distributions on cirrus clouds determined from SAGE data. *J. Geophys. Res.*, **91,** 2775–2785.

Yamanouchi, T., and S. Kawaguchi, 1992: Cloud distribution in the Antarctic from AVHRR data and radiation measurements at the surface. *Int. J. Remote Sens.*, **13,** 111–127.